ADVANCED MATERIALS TECHNOLOGIES
www.advmattechnol.de

Multifunctional Skin-Inspired Flexible Sensor Systems for Wearable Electronics

*Kaichen Xu, Yuyao Lu, and Kuniharu Takei**

Skin-inspired wearable devices hold great potentials in the next generation of smart portable electronics owing to their intriguing applications in healthcare monitoring, soft robotics, artificial intelligence, and human–machine interfaces. Despite tremendous research efforts dedicated to judiciously tailoring wearable devices in terms of their thickness, portability, flexibility, bendability as well as stretchability, the emerging Internet of Things demand the skin-interfaced flexible systems to be endowed with additional functionalities with the capability of mimicking skin-like perception and beyond. This review covers and highlights the latest advances of burgeoning multifunctional wearable electronics, primarily including versatile multimodal sensor systems, self-healing material-based devices, and self-powered flexible sensors. To render the penetration of human-interactive devices into global markets and households, economical manufacturing techniques are crucial to achieve large-scale flexible systems with high-throughput capability. The booming innovations in this research field will push the scientific community forward and benefit human beings in the near future.

1. Introduction

The everlasting pursuit of preferable human life propels the ceaseless advances of intelligent community. In particular, the burgeoning concept of Internet of Things (IoTs) is revolutionizing the way we live our lives through active interaction with smart network. As the kernel of IoTs, wearable electronic skin (E-skin) devices take the predominant role in seamlessly interfacing among surroundings and individuals by virtue of integrated flexible sensor systems based on wireless network connectivity. Huge efforts, in the past decade, have thus been dedicated to developing versatile human-interactive devices via imitating skin-like functions, such as tactile, humidity, or temperature sensing capabilities, contributing to diverse intriguing applications (e.g., soft robotics, medical devices).[1–6] Despite state-of-the-art bulk-based planar integrated-circuit devices, their rigid and brittle nature gives rise to the incompatibility with curvilinear and soft human bodies, restricting the development of newborn human-friendly interactive electronics. In contrast, the bendable and flexible wearable electronics could be conformally attached onto human bodies almost without discomfort and succeed in performing a great deal of sensing functionalities. Realization of such promising goals requires the flexible sensor platforms provided with crucial characteristics of light weight, ultrathinness, superior flexibility, stretchability, high sensitivity as well as rapid response.[7–10] Inspired by the perceptive features of human skins, the wearable sensor systems are capable of acquiring abundant information from the external environment with the assistance of sensing modules, such as pressure sensors, strain sensors, temperature sensors, etc.[11] A typical example is their application in prosthetics that could afford the capacity to perceive touch or temperature for the disabled.[12] Additionally, the wearable sensor systems are able to identify physical or chemical signals produced by the human body, providing promising opportunities to evaluate health states.[5,13–15]

Conventional skin-like sensor platforms primarily comprise one or two sensing modules, data processing units, and power supplies. Their unitary functionality, however, cannot satisfy the increasing demands of IoTs. Recently, the rapid advances in novel sensing materials, fabrication strategies, and innovative electronic constitution contribute to the development of versatile integration of multimodal sensors, which could synchronously distinguish diverse stimuli from the complex environment and monitor multiple vital signs from the human body.[16,17] In spite of several attempts done in terms of such multimodal sensor systems, one of the cumbersome issues originates from the crosscoupling effect among different categories of signals simultaneously generated by various sensors. Furthermore, the skin-like multiple sensor systems usually suffer from the limited number of repeated use, resulting in their high use-cost. The development of separable versatile devices may address this issue with one layer realized by cost-effective materials and fabrication manners for disposable use and the other composed of relatively expensive components for repeatable applications.[18] Additionally, the multiple bending or

Dr. K. Xu, Y. Lu, Prof. K. Takei
Department of Physics and Electronics
Osaka Prefecture University Sakai
Osaka 599-8531, Japan
E-mail: takei@pe.osakafu-u.ac.jp
Prof. K. Takei
JST PRESTO
Kawaguchi, Saitama 332-0012, Japan
The ORCID identification number(s) for the author(s) of this article can be found under https://doi.org/10.1002/admt.201800628.

DOI: 10.1002/admt.201800628

 © 2019 WILEY-VCH Verlag GmbH & Co. KGaA, Weinheim

stretching processes often lead to performance degradation of flexible sensors, especially in harsh working environment, enabling the inaccurate measurement of signals, and increasing the electronic waste streams. Fortunately, the spontaneous restorative nature of human skin inspires us to develop self-healable materials as the backbone of the devices, allowing the human–machine interfaces to self-repair upon damages through nonautonomic or autonomic processes.[19] However, the vast majority of current self-healable devices have the capability to be only partially self-healed, and most importantly, it is still a formidable challenge to integrate functional multimodal sensors into the self-healable matrix. Another significant aspect of flexible sensor systems lies in power modules, which are usually bulky, rigid, and incompatible with the emerging multifunctional E-skin systems. The promising alternative strategy of flexible self-powered systems render the possibility to concurrently drive a couple of sensors via harvesting the ubiquitous energy from the structured environment or the human body itself.[20] To realize the full potential of wearable IoTs, it is critical to develop self-powered sensor patches that simultaneously measure multiple physiological cues (e.g., cardiac, sweat, respiratory) with high repeatability and accuracy. In addition, the widespread application, especially in resource-limited environment, of the intelligent wearable sensors require them to be realized over large scales with economic fabrication approaches.[21] Particularly, the on-demand and multiple-spot measurement of signals prompts the development of flexible sensor arrays endowed with in vivo mapping capabilities.[22–24]

In this review, we present the latest advances of multifunctional skin-inspired flexible wearable sensor platforms for healthcare monitoring and soft robotic applications. First, the recent successful demonstrations of strain/pressure, temperature, chemical and optical sensors are briefly overviewed and their challenges are critically analyzed. The second section highlights the emerging multifunctional wearable sensor systems in detail, categorized into three main subfields: i) integration of multimodal sensors, ii) self-healing material-based flexible devices, and iii) self-powered flexible sensors (**Figure 1**). Additionally, the large-scale flexible sensor systems are described, aiming at permeating into global markets and households. Finally, the future trends of multifunctional skin-like sensing systems are provided.



Kaichen Xu received his Ph.D. degree from the Department of Electrical & Computer Engineering at National University of Singapore in 2018 and his B.Sc. from Nanjing University of Posts and Telecommunications in 2014. Currently, he is a postdoctoral fellow at Osaka Prefecture University in Japan under Prof. Kuniharu Takei. His research interests include multifunctional flexible sensors for soft robotic applications and healthcare monitoring.



Yuyao Lu received her M.Sc. degree from the Department of Chemistry at National University of Singapore in 2018 and her B.Sc. from Suzhou University of Science and Technology in 2017. Currently, she is a research assistant at Osaka Prefecture University in Japan under Prof. Kuniharu Takei. She is focused on the synthesis of novel nanomaterials for flexible sensors.



Kuniharu Takei received his Ph.D. degree from Toyohashi University of Technology in Japan in 2009. After working as a postdoctoral fellow at the University of California, Berkeley from 2009 to 2013, he joined the faculty of Osaka Prefecture University in Japan. Currently he is an associated professor in the Department of Physics and Electronics. His contributions are to develop multifunctional high-performance flexible and wearable devices using printable inorganic materials.

2. Various Categories of Flexible Sensors

2.1. Strain and Pressure Sensors

Pressures sensors, also known as tactile/strain sensors, have attracted a number of research attentions in recent years, especially for skin-based electronic devices.[32–36] Owing to their distinct merits of flexibility, durability, biocompatibility as well as lightweight, flexible strain, and pressure sensors are able to be tightly adhered onto the human skin for the real-time monitoring of physiological health, such as heart rate or respiratory rhythm. To realize the high-performance skin-inspired sensors, a great diversity of highly sensitive sensor systems have been reported through rationally engineering functional nanomaterials or hybrid micro/nanostructures based on effective transduction mechanisms through converting external stimuli into electrical signals.[33,34,37–40] These transduction methods generally include piezoresistivity, piezoelectricity, and capacitance. For the detailed illustration of these mechanisms, interested readers may refer to the excellent review by Rim et al.[41] Among them, piezoresistivity is considered as the most common one owing to their comparatively facile system designs and readout mechanisms via transducing force variations into resistance change. In the past decade, enormous

© 2019 WILEY-VCH Verlag GmbH & Co. KGaA, Weinheim

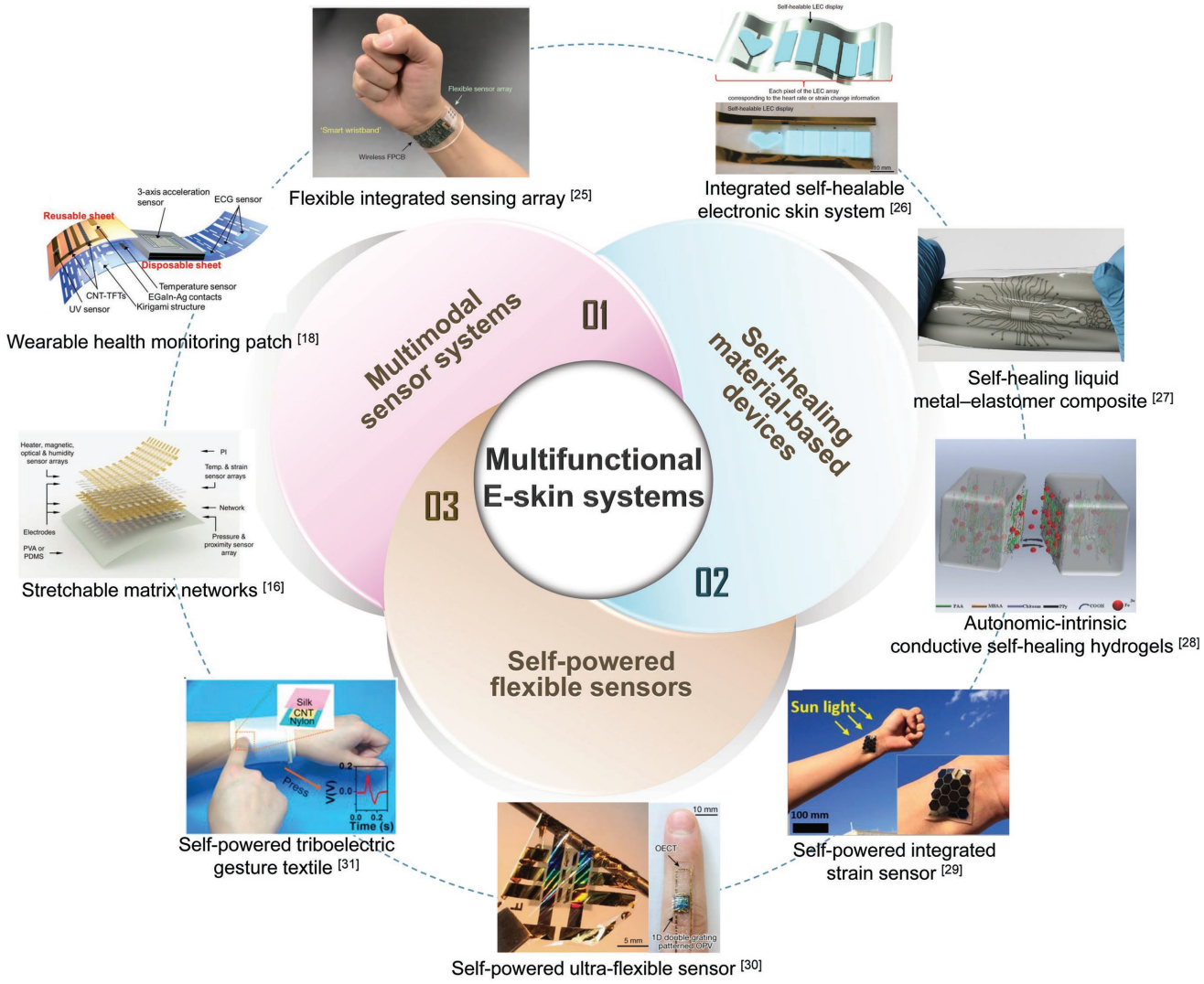


Figure 1. Toward multifunctional E-skin systems. Multimodal sensor systems: stretchable matrix networks. Reproduced with permission.[16] Copyright 2018, Nature Publishing Group. Wearable health monitoring patch. Reproduced with permission.[18] Copyright 2016, American Association for the Advancement of Science. Flexible integrated sensing array. Reproduced with permission.[25] Copyright 2016, Nature Publishing Group. Self-healing material-based devices: integrated self-healable electronic skin system. Reproduced with permission.[26] Copyright 2018, Nature Publishing Group. Self-healing liquid metal–elastomer composite. Reproduced with permission.[27] Copyright 2018, Nature Publishing Group. Autonomic–intrinsic conductive self-healing hydrogels. Reproduced with permission.[28] Copyright 2017, John Wiley & Sons. Self-powered flexible sensors: self-powered integrated strain sensor. Reproduced with permission.[29] Copyright 2018, Elsevier B.V. Self-powered ultraflexible sensor. Reproduced with permission.[30] Copyright 2018, Nature Publishing Group. Self-powered triboelectric gesture textile. Reproduced with permission.[31] Copyright 2018, American Chemical Society.

efforts have been concentrated in improving the parameters of wearable strain devices, such as sensitivity, gauge factor (GF), linearity, hysteresis, response, and recovery time as well as overshoot behavior.[42] Nevertheless, other device performances should also be taken into concern if state-of-the-art flexible pressure sensors are expected. For instance, it is hard to accurately measure the pressure under dynamic deformation because of the variable sensing performance induced by mechanical deformation. To address this challenge, Someya and co-workers unprecedentedly developed a bending-insensitive, ultraflexible, and resistive-type pressure sensor with composite nanofibers as building blocks.[43] Significantly, the sensor properties remain unvaried even though the bending radius of the sensor drops down to 80 μm owing to the thin substrate (thickness: <2 μm) as well as entangled nanostructure (**Figure 2**a). This results in precisely measuring the distribution of the normal pressure on 3D surfaces and the performance variation is negligibly small before and after wrapping devices around an injection needle (Figure 2b–d). In the following part, two emerging categories of wearable strain devices are briefly overviewed regarding to memorable tactile sensors as well as acceleration sensors.

The majority of skin-inspired strain sensors are unable to retain tactile information after removing external force. To enhance the versatility of state-of-art E-skin based systems, the wearable pressure sensors coupled with memory characteristic have been demonstrated by several research groups.[46–48]

© 2019 WILEY-VCH Verlag GmbH & Co. KGaA, Weinheim

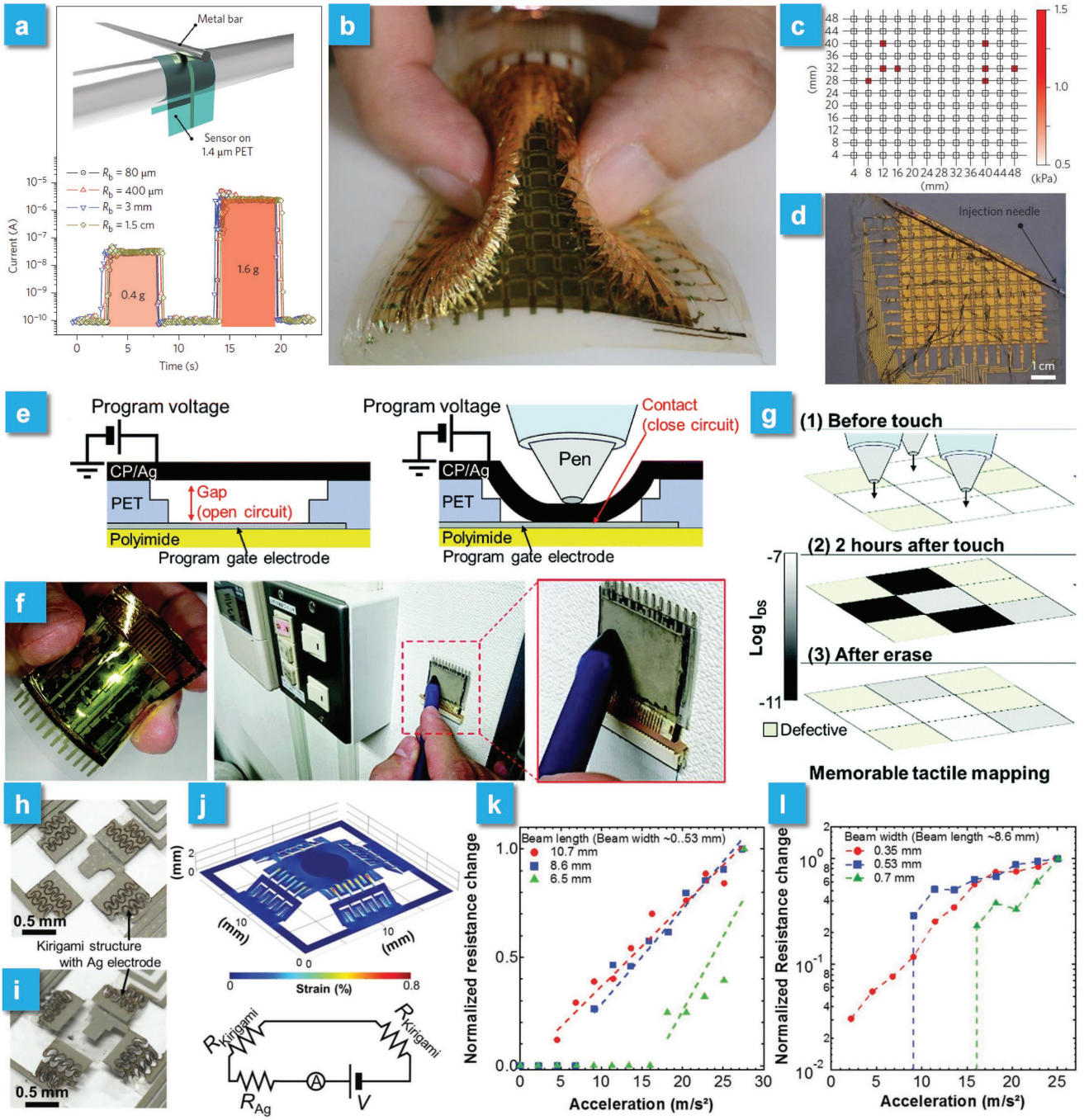


Figure 2. a) Tested pressure response of the device in the bent state and response of the device fabricated on a 1.4 μm thick PET substrate. b) Photograph of an integrated sensor array attached to the surface of a soft balloon, to which a pressure was applied by a pinching motion. c) Measured pressure data distribution under complex bending, showing no pressure signal from deformation such as wrinkling. d) Photograph of a sensor wrapped around an injection needle. a–d) Reproduced with permission.[43] Copyright 2016, Nature Publishing Group. e) Tactile touch sensor and programming mechanism of FGRAM without (left) and with (right) applying a touch. f) Photo of the fabricated device and demonstration image of the e-wallpaper. g) Memorized touch information array 1) before touch, 2) 2 h after touch, and 3) after erasing the touch information. e–g) Reproduced with permission.[44] Copyright 2017, Royal Society of Chemistry. Photos of kirigami electrodes h) before and i) after stretching. j) FEM simulation of the kirigami structure with a 2 mm stretching displacement (top) and equivalent circuit for the resistance measurements of kirigami electrodes under stretching (bottom). Normalized resistance changes for k) different *L* values and l) beam width. h–l) Reproduced with permission.[45] Copyright 2017, John Wiley & Sons.

Similar to synapses among neurons, the flexible memory sensor could be applied to imitate the brain's memory functionality to store analogue value.[49] For example, through replacing the bottom electrodes of pressure sensors with top electrodes arrays in memory devices, flexible haptic memory devices are realized.[46] The applied strain can be maintained for more than

© 2019 WILEY-VCH Verlag GmbH & Co. KGaA, Weinheim

one week with little decay. Furthermore, Casula et al. demonstrated an organic, nonvolatile resistive memory device based on organic pressure-sensitive elements.[48] High retention time with at least 6 months is achieved. However, realization of a practical and commercial flexible pressure sensor-memory still faces enormous challenges. Takei et al. reported a flexible tactile touch memory array for electronic wallpaper (e-wallpaper) based on a flexible resistive-change nonvolatile floating gate random access memory (FGRAM) array (Figure 2e).[44] Due to its promising capability to realize integrated circuits on macroscale substrates, InGaZnO thin-film transistors (TFTs) are employed as FGRAMs for flexible pressure sensors array. The value of such an e-wallpaper, for example, lies in its ability to memorize touch information like a message board (Figure 2f,g). Without a touch, the program voltage is disconnected with the gate electrode of the FGRAM. After applying a tactile touch onto the sensor, the program voltage is supplied to the FGRAM with the positive shift of threshold voltage. It is demonstrated that after two hours by applying the pressure using three pens over the device, the information is still maintained, which can be refreshed by triggering −15 V erasing voltage. Through the incorporation of temperature sensors, the room temperature can be memorized and controlled.

Until now, most of the skin-inspired wearable strain sensors are used to monitor heartbeat or respiration rates, which are highly associated with illness. Another kind of equally vital applications of wearable strain sensors are their capability to monitor physical movement and motion. Despite the immense advances in monitoring health conditions by diverse wearable sensors, the detection of health information alone allows no sufficient analyses to fully predict or diagnose diseases. As a matter of fact, the recorded health conditions, such as skin temperature or electrocardiogram (ECG), are strongly related to the subject's physical activity. Simultaneous detection of human activity/motion is thus of paramount importance. Typical examples of motion sensors rely on the flexible strain sensors attached onto the fingers or knee joints to monitor their movement.[50–54] Nevertheless, limb movements are not always correlated with overall physical activities, hence resulting in probably inaccurate diagnosis in combination with the recorded health data. Inspired by the kirigami structure, a three-axis acceleration sensor was developed composed of four beams integrated with three strain sensors in response to changes in structural strain (Figure 2h–j).[18,45] The introduction of kirigami structure hinders the stretching induced mechanical and electrical failures and meanwhile improves the comfort for wearers. It is found that the threshold acceleration of the motion sensor is about 5–12 m s^{-2}, determined by the direction of acceleration.[18] Through the rational tuning of structural dimensions, a sufficiently low acceleration threshold less than 3 m s^{-2} is obtained at the beam length (L) of 10.7 mm and width (W) of 0.35 mm, enabling its possibility to detect light human activity, such as small steps (Figure 2k,l).[45] To make the acceleration sensor adaptable to a wide range of people, the further device developments are demanded to obtain desired detectable threshold ($D_{\text{Threshold}}$) based on the following relationship

$$D_{\text{Threshold}} \propto L^{2.7}/W \quad (1)$$

Through the incorporation of such motion/acceleration sensors into more functional flexible devices, the simultaneous monitoring of physical activity, skin temperature, ECG, UV exposure, etc., could be realized.

2.2. Temperature Sensors

Body temperature, as a basic index in physiology, is a significant indicator of many symptoms, such as insomnia, fever, depression, or metabolic functionality, providing abundantly useful medical diagnostic information. Real-time and accurate measurement of localized temperature changes is very important. Traditional medical examination generally relies on periodic measurement of body temperature by thermometers. In contrast, the emerging wearable temperature measurement systems can be conformally attached onto human skins with minimal user awareness for continuous healthcare monitoring.[55] High sensitivity, fast response, good reliability, wide-working temperature range as well as light weight of the flexible temperature sensors is highly desired. This real-time health condition monitoring may find unusual change of condition in advance related with some signals for disease. Real-time monitoring increases the chance to find this sign compared to the conventional periodic measurements. Most flexible temperature sensors are in operation based on the change of resistance, which is usually implemented by homogeneously spreading conductive fillers into insulative polymer matrix or heterogeneously creating temperature-sensitive conductors on flexible substrates. For example, Chen et al. reported a soft thermal sensor through the combination of single-wall carbon nanotubes composed of carboxyl groups with polymers based on hydrogen bonds.[56] The flexible thermal sensor is endowed with superior mechanical adaptability due to rich noncovalent hydrogen bonds of polymers. Takei et al. demonstrated a temperature sensor by mixing a conductive poly(3,4-ethylenedioxythiophene):poly(styrenesulfonate) (PEDOT:PSS, 1.3 wt% in water) (Sigma Aldrich, USA) and a carbon nanotube (CNT) paste (SWeNT, USA) with a 10:1 weight ratio, followed by printing on flexible substrates.[57,58] The temperature sensitivity of around 0.61% $°C^{-1}$ is obtained, which is slightly better than that of Pt thermal sensor.[59] To further increase the sensitivity and improve response time, it has been found that positive temperature coefficient (PTC) composites are alternative candidates as the backbone materials to construct flexible temperature sensors with prominent capacity to exhibit six orders of magnitude of only 5 °C or less.[60] High resolution of 0.1 °C or less near body temperatures and fast response time of 100 ms are achieved, which realizes the measurement of dynamic change of temperature in the lung during very quick artificial respiration.

Besides the criteria of flexible temperature sensors mentioned above, other properties should also be taken into considerations, such as response to subtle change of working environment, cross-sensitivities (e.g., strain) or scalable sensors array with mechanical stretchability. Several attempts have been made to address these issues. For instance, via integrating the temperature sensitive material with a semipermeable polyurethane film, a stretchable and breathable temperature sensor

© 2019 WILEY-VCH Verlag GmbH & Co. KGaA, Weinheim

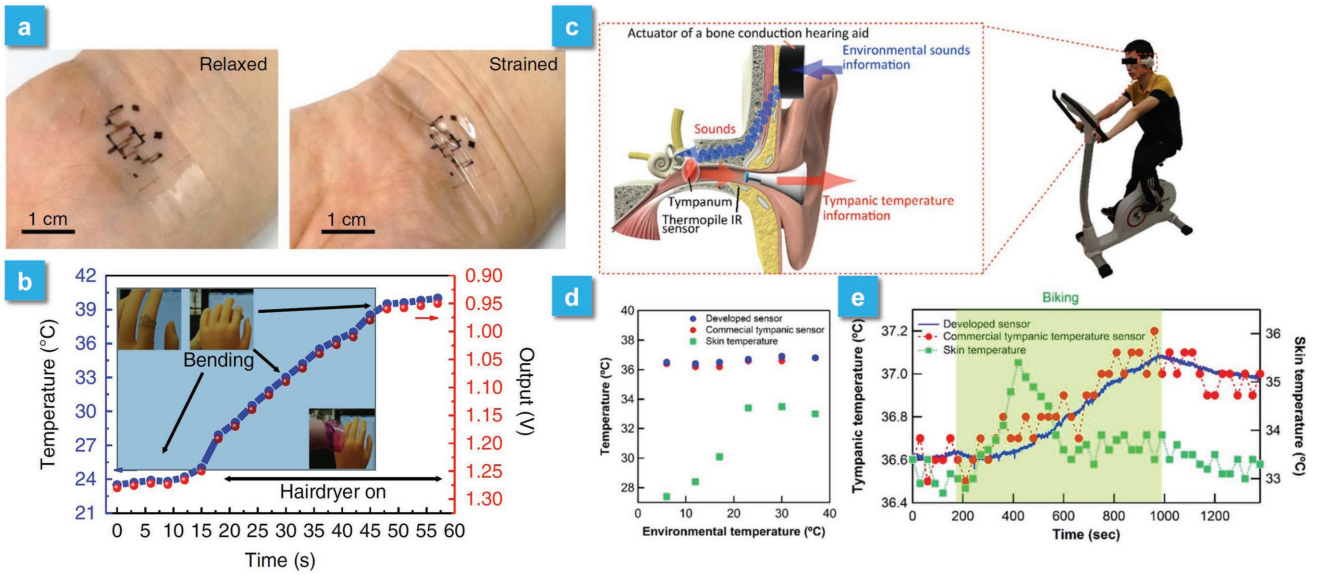


Figure 3. a) Optical photograph showing the conformability of the temperature sensing circuit. The photograph highlights the skin-like nature of the intrinsically stretchable temperature sensor attached on the medial aspect of the wrist (left), and laminated to the skin during wrist bending (right). b) Demonstration of the stretchable temperature sensor attached to the knuckle area of a flexible rubber prosthetic hand. The temperature sensor showed stable functionality during repeated bending. a,b) Reproduced with permission.[62] Copyright 2018, Nature Publishing Group. On-body tests using the 3D printed earable smart device. c) Schematic diagram of the smart device operation. d) Skin and core body temperatures as a function of environmental temperature. e) Skin and core body temperature change during biking. c–e) Reproduced with permission.[64] Copyright 2017, American Chemical Society.

was proposed with the capability to reflect subtle temperature change caused by water dropping and wind blowing.[61] To circumvent the cross-sensitivity and accurately measure electrical output of stretchable temperature sensors, Zhu et al. demonstrated static and dynamic differential voltage readout strategies, leading to the absolute inaccuracy of the output within ±1 °C under uniaxial strains, although this inaccuracy could be further improved in future (**Figure 3**a,b).[62] The stable functionality of temperature sensors allows the precisely real-time monitoring during rapid stretching cycles. In addition, the increasing demand of dynamically monitoring temperatures on multipoints of curved surfaces is in need of scalable temperature sensor network.[63] The detailed illustration will be presented in Section 4.

Conventional skin-based temperature sensors are targeted at measuring the skin temperature. Such sensors, however, are usually affected by ambient conditions, such as humidity or ambient temperature, resulting in imprecisely acquiring health status of human bodies. In order to measure the true body temperature accurately, the measurement of core-body temperature is one of the excellent strategies. Javey and co-workers invented a wearable "earable" device, which can be worn on the ear to realize real-time monitoring of core-body temperature through the tympanum based on an infrared sensor (Figure 3c).[64] The experimental results indicate that with the rise of environmental temperature, the core-body temperature almost keeps constant, while the skin temperature is strongly affected (Figure 3d,e). In addition, during the exercise, the core-body temperature increases steadily up to around 37 °C, while the skin temperature quickly rises up to nearly 35 °C before dropping back down at the end of biking. The drop in the skin temperature is probably attributed to perspiration during the exercise. The results of the earable core-body temperature sensor is in excellent agreement with that measured by a commercial tympanic sensor, indicating its promising roles in precisely real-time monitoring individual's health and physiological state.

2.3. Chemical Sensors

Flexible chemical sensors are capable of in situ monitoring of the human health via rapid detection of biomarkers from the human body. Different from the majority of flexible sensors that aim to gain the information of physical activities or vital signs, chemical sensors provide a more straightforward manner for noninvasive personal health monitoring at the molecular level. In the past several years, a plurality of body fluids have been employed for healthcare diagnostics by flexible wearable chemical sensors, such as saliva, breath, blood, sweat, etc.[13] For example, a bio-interfaced sensing platform composed of hybrid graphene/electrode/silk structure was reported for chemical and biological sensing.[65] Via transferring the flexible sensors onto tooth enamel, the flexible sensor is able to recognize *H. pylori* cells in human saliva with a detection limit of around 100 cells. Nevertheless, the acquired information of saliva sensors is usually influenced by dietary habit, providing restricted physiological insight. Regarding to breath analyses, rich volatile organic compounds (VOCs) are contained in exhaled breath, which affords an effective route for safe screening. Kahn et al. demonstrated a flexible nanoparticle (GNP) sensor that could collect resistance data in real-time under bending and exposure thanks to the good response of sensor varying with the type

© 2019 WILEY-VCH Verlag GmbH & Co. KGaA, Weinheim

of VOCs and their concentrations.[66] This enables the examination of breath VOCs for the diagnosis of ovarian cancer. However, the biomarkers exhaled from breath may suffer from the interference from humidity or contamination from ambient air. Additionally, blood diagnostics can be performed by implantable sensors, but it is hard to realize noninvasive measurement based on wearable platforms. On the contrary, sweat-based sensors present various advantages over other body bio-fluids sensing because of their on-demand and continuous monitoring capabilities at one's convenience.

As an important category of bio-fluid, sweat contains abundant biochemical markers (e.g., glucose, lactate, sodium, and potassium), which are highly associated with our physiological states. The timely, accurate and sensitive monitoring of sweat ensures early diagnostics of relevant diseases. Current research focuses on flexible sweat sensors in developing effective sweat sampling solutions and high-performance sensitive sensing systems on flexible matrix. Various wearable platforms have been demonstrated, such as temporary tattoos, patches, or wrist-bands.[69] Among a variety of architectures for wearable sweat sensors, microfluidic-based sweat systems are one of the most promising strategies owing to their shorter sweat sampling and filling times.[67,70–73] Koh et al. developed a stretchable microfluidic system with the capability to be intimately and robustly bonded to the skin surface (**Figure 4**a–c).[67] The sweat could be harvested from pores on the skin surface and then delivered to different channels and reservoirs, rendering the colorimetric detection of sweat loss, pH, lactate, chloride as well as glucose concentrations. Furthermore, a skin-mounted microanalytical flow system was reported via integrating of an innovative microfluidic configuration and electrochemical flow detectors.[71] However, most of these wearable sweat sensors rely on exercise to extract sufficient amount of sweat from the skin surface, preventing their universal applications. An electrochemically enhanced iontophoresis interface could surmount this issue through incorporation into a wearable sweat sensing system (Figure 4d,e).[68,74] The sweating could be stimulated locally via iontophoresis, allowing the medical screenings under sedentary circumstances. Although enormous advances have been made in skin-like wearable sweat sensors, only small molecules or ions have been extracted and measured by in situ monitoring, while the excretion of larger biomolecules such as proteins, DNA, RNA, etc., from sweat have not been clearly comprehended, which may demand related biologists to be involved in this research field.

2.4. Optical Sensors

Optical sensors are a wide range of devices with the capability to detect a variety of light properties, such as wavelength, frequency, intensity, or polarization. One type of devices relies on the conversion of light with broad bandwidth into electrical signals.[75–77] The performance of the optical sensors can be

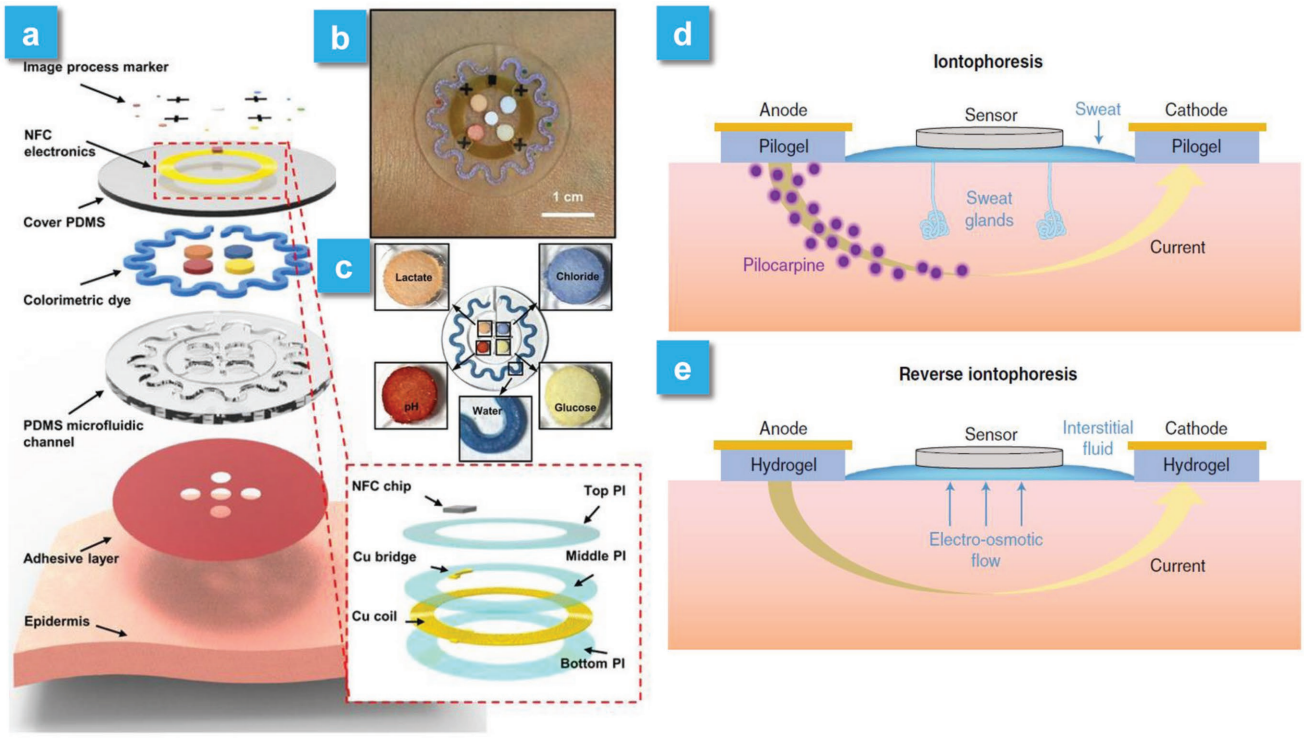


Figure 4. a) Schematic illustration of an epidermal microfluidic sweat monitoring device and an enlarged image of the integrated near-field communication (NFC) system (inset). b) Optical image of a fabricated device mounted on the forearm. c) Colorimetric detection reservoirs that enable determination of different analytes. a–c) Reproduced with permission.[67] Copyright 2016, American Association for the Advancement of Science. d) Iontophoresis relies on topical current application for local sweat stimulation. Current is applied between pilogels, or hydrogels containing the sweat-stimulating drug pilocarpine. e) Reverse iontophoresis uses current application to electro-osmotically drive interstitial fluid through the epidermis to the skin surface. d,e) Reproduced with permission.[68] Copyright 2018, Nature Publishing Group.

© 2019 WILEY-VCH Verlag GmbH & Co. KGaA, Weinheim

evaluated by various indicators, including selectivity, sensitivity as well as response time.[78] In healthcare diagnostics, one of the most popular optical sensors are based on photodetectors, which are applied for pulse oximeters generally composed of two light-emitting diodes (LEDs) with different emission wavelengths and a photodetector. The LEDs are usually placed on a thin part of the patient's body and the light transmitted or reflected in the tissue is then detected by the photodetector, which is placed beside or opposite the LEDs (reflected or transmitted modes). Currently, the commercial pulse oximeters are composed of bulky and rigid integrated circuits with high large-area scaling cost, limiting their practical applications in noninvasively measuring human pulse and tissue oxygenation, especially when the wearer is on the move. The development of high-performance flexible optoelectronic systems thus play a vital role in healthcare monitoring.

Driven by the aforementioned challenges, Arias and coworkers demonstrated an organic optoelectronic pulse oximetry sensor on a plastic substrate, consisting of green (532 nm) and red (626 nm) organic LEDs (OLEDs) coupled with organic photodiodes (OPDs) at the transmitted mode.[79] Through the processes of systole and diastole, arterial oxygen saturation can be calculated due to different light absorptivities of oxyhemoglobin (HbO_2) and deoxy-hemoglobin (Hb) at red and green wavelengths. 1% error for pulse rate and 2% error for oxygenation are achieved when comparing the flexible organic sensor with the inorganic sensor. Nevertheless, the relatively thick plastic substrate with high Young's modulus in this work cannot enable the devices to be seamlessly laminated onto the skin imperceptibly. Significantly, an ultrathin and ultraflexible reflective pulse oximeter comprising polymer LEDs (PLEDs) and an organic photodetector (OPD) was successfully developed by Someya and co-workers.[80] To realize such a smart E-skin system, a high-quality ultrathin passivation layer composed of five alternating inorganic (SiON) and organic (Parylene) layers by plasma-enhanced chemical vapor deposition (CVD) is employed for their ultraflexible organic optoelectronic devices. The total thickness of the devices is only 3 μm, including the substrate and encapsulation layer. After laminating the pulse oximeter on a finger, the oxygen concentration of blood is measured (**Figure 5**a–c). It is envisioned that such ultrathin flexible optical sensors can be directly laminated on organs for the blood oxygen level monitoring during and after surgery. Furthermore, in order to drive the light into a deeper penetration skin depth and pick up signals from larger arterioles, near infrared (NIR) light with low attenuation is considered to be more suitable for skin-based devices for health monitoring.[81,82]

Another category of optical sensors is plasmon-enhanced optical sensing, which is generally built from judiciously tailored plasmonic nanostructures, rendering the enhancement or modulation of optical signals possible, such as spectral-shifts based plasmonic sensors,[84] plasmon-enhanced fluorescence sensors,[85] and surface-enhanced Raman scattering (SERS) sensors, etc.[86] Particularly, SERS has attracted intensive research attentions due to its capability to provide fingerprint information of analytes with narrow spectral peaks.[87] To achieve high-performance SERS substrates, it is crucial to deliberately engineer uniform large-scale plasmonic nanostructures with high-density of "hot-spots," allowing the generation of enhanced electric fields as large as possible.[88–92] Huge efforts, in the past decades, thus have been dedicated to exploiting versatile SERS platforms by rational chemical syntheses or advanced lithographic routes in aqueous solutions or on rigid substrates.[93–99]

Especially, in recent years, the SERS systems constructed from soft/flexible materials have drawn increasing attentions owing to their distinct merits for real-time point-of-care (POC) diagnostics. Currently, the flexible SERS platforms are primarily classified into i) actively tunable SERS, ii) swab-sampling strategy as well as iii) in situ SERS monitoring means.[83,100,101] Among them, the in situ SERS detection based on the flexible substrates is considered as the most promising approach, which is performed by first conformally attaching the flexible SERS substrates onto objective surfaces of interest, followed by the excitation of incident photons and collection of Raman signals from the back side of the SERS substrates. Until now, a diversity of flexible substrates have been applied for in-situ SERS detection, such as PDMS,[102] PMMA,[103] polyethylene terephthalate (PET),[104] polyethylene (PE),[105] poly(vinylpyrrolidone) (PVP),[106] paper,[107] adhesive tape,[108] as well as nanowires.[109] The conventional methods to prepare active nanostructures on flexible and transparent substrates rely on depositing nanoparticles by physical or chemical routes. Particularly, the implementation of uniform nanostructures generally involves the state-of-art lithographic techniques and then pattern transfer processes. To explore a facile, yet efficient method to fabricate homogeneous nanostructures on the flexible substrates over a large area for the in situ SERS detection, Xu et al. developed a biocompatible and biodegradable SERS substrates via irreversibly and uniaxially stretching metal deposited flexible poly (ε-caprolactone) (PCL) surface plasmon resonance (SPR) film as wearable sensors for in situ detection of analytes (Figure 5d).[83] The PCL film, as an excellent flexible, biodegradable, and biocompatible material with good transparency (≈90%) and temperature stability (9.62%), is for the first time employed as a building block for flexible SERS substrates. After the deposition of Ag film, the composite film after stretching exhibits surprising phenomena: three dimensional and periodic wave-shaped microribbons array embedded with a high density of nanogaps functioning as hot-spots at an average gap size of 20 nm and nanogrooves array along the stretching direction (Figure 5e). The stretched polymer surface plasmon resonance film gives rise to more than 10 times signal enhancement in comparison with that of the unstretched composite film due to the localized fields within the nanogaps and nanogrooves (Figure 5f). The ultrathin flexible SPR film (≈10 μm) affords an intriguing way to not only in situ detect molecules on curved surfaces, but also noninvasively monitor glucose level and other intractable diseases through the swab-sampling of fresh human tears for healthcare monitoring (Figure 5g–i).

3. Multifunctional Skin-Interfaced Wearable Devices

The vision of human-interactive wearable devices is to imitate or even surmount the perceptive capabilities of human skin, such as temperature and tactile sensing properties. Additional functionalities, such as chemical or optical sensing capabilities,

© 2019 WILEY-VCH Verlag GmbH & Co. KGaA, Weinheim

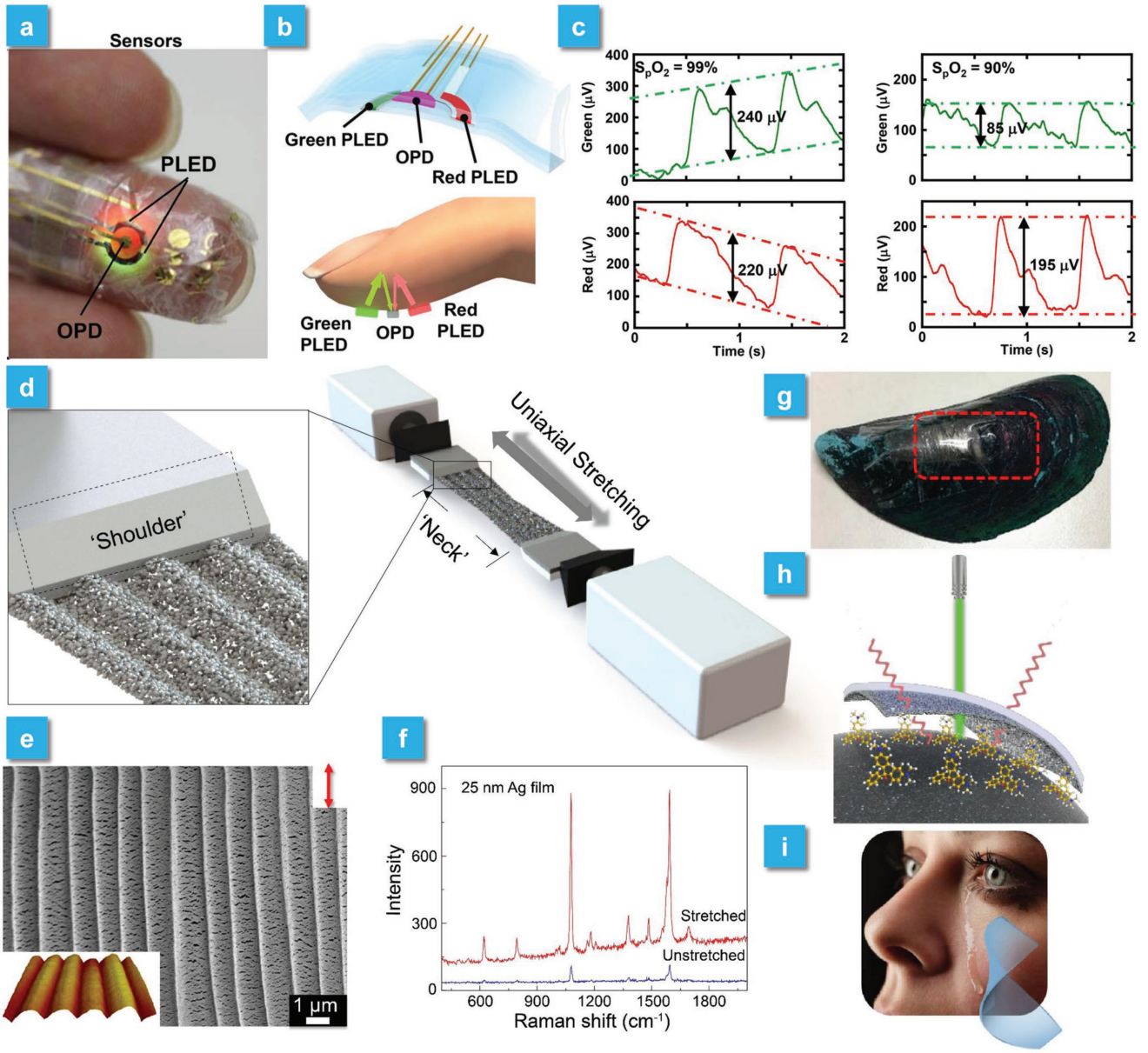


Figure 5. a) Photograph of a finger with the ultraflexible organic optical sensor attached. b) Device structure of the pulse oximeter (top) and operation principle of the reflective pulse oximeter (bottom). c) Output signal from OPD with 99% (left) and 90% (right) oxygenation of blood. a–c) Reproduced with permission.[80] Copyright 2016, American Association for the Advancement of Science. d) The uniaxial stretching of polymer SPR film at a constant stretching speed. e) Surface morphology of stretched polymer SPR film with 25 nm Ag film. The arrows denote the direction of externally applied stress. f) SERS spectra of 4-methylbenzenethiol molecules adsorbed on polymer SPR film with 25 nm Ag film. g) A photograph image of polymer SPR film attached onto the green mussel surface contaminated by malachite green molecules. h) Schematic diagram of contacting polymer SPR film onto the green mussel and collecting the SERS signals from the back side surface. i) Schematic of collection of fresh human tears by polymer SPR film for healthcare monitoring. d–i) Reproduced with permission.[83] Copyright 2017, American Chemical Society.

are also considered to be incorporated beyond skin functionalities. In order to reach this ambitious goal, the further study of skin-interfaced systems is encouraged to be transited from "one system = one result" to "one system = several results." This will endow the health-monitoring systems with plentiful functionalities to acquire diverse vital signs (temperature, heart rate, respiratory rhythm, oximeters, physical activities, etc.) within only a single device.[5] Furthermore, one of the most intriguing properties of human skin is its natural ability to recover from injury. However, most of the current skin-interactive systems usually suffer from device performance degradation over time owing to multiple bending or stretching operations. Fortunately, to obtain such distinctive feature of human skin, self-healable materials have recently driven crucial advances by means of imitating restorative characteristics of human skin to hold the capability of self-repair behaviors, which enables the

© 2019 WILEY-VCH Verlag GmbH & Co. KGaA, Weinheim

deformable electronics to recover its stretchability or prevent permanent breakdowns.[110] Additionally, to synchronously manipulate these multiple flexible sensors, including signals' processing and transmission, the power supply, however, is a formidable issue. Conventional power sources and energy storage systems are usually bulky with circuital connections and demand frequent charging and replacement, which strongly restricts their practical applications. To catch up with the trend of lightweight, ultrathin, and user-friendly skin-interfaced wearable devices, innovative energy supply systems are urgently required. A promising alternative strategy to resolve the issue of energy supplies in E-skin is to develop functional self-powered systems, which not only provide the desired sensing functionalities, but also can work under the circumstances of no external power supplies.[111] In pursuit of state-of-the-art multifunctional skin-interfaced wearable health-monitoring systems, in this part, we will primarily concentrate on discussing the latest developments of the foregoing aspects.

3.1. Integration of Multiple Sensors

In the past decade, a number of attempts have been continuously involved in boosting the performance of various flexible sensors in terms of monitoring subjects' physical or chemical states, such as temperature, motion, heartbeat, sweat, etc. Nevertheless, most of these flexible devices are usually able to gain one sole vital sign, which is insufficient to diagnose health conditions. One alternative route relies on the transduction of various stimuli into a coupled signal within a single device, but it mostly suffers from the interference of multiple signals in the decoupling procedure.[112,113] Additionally, the output of a specific flexible sensor is usually influenced by other physiological information. For example, sweat contains rich clinical information, such as glucose, calcium, potassium, metal ions, or pH, but their value is highly dependent on the variation of skin temperature.[25,114] Thus, the incorporation of multiple sensors into a single chip is of high significance to synchronously detect multicomplex stimuli from the skin, rendering the accurate and selective diagnosis of various diseases.

In spite of many existing challenges, a plurality of research groups have taken the first step toward merging at least two categories of sensors into a flexible device.[112,115–117] Particularly, the integration of temperature and pressure/strain sensors has attracted massive attentions, which was pioneered by Someya et al.[118] One of the major concerns is to simultaneously measure multiple signals without crosscoupling. A general strategy relies on stacking double active layers as bimodal sensors to monitor the temperature and pressure stimuli, respectively. For instance, Jeon et al. demonstrated a vertically stacked bimodal device configuration based on separation between piezoresistive effect and thermoelectric effect, avoiding decoupling the data.[115] Taking advantage of the superior electrical, mechanical, and lightweight features of carbon materials, an integrated temperature-pressure E-skin was reported with silk-nanofiber-derived carbon fiber membranes as both active materials, which exhibits a temperature sensitivity of 0.81% per centigrade and an extremely high sensitivity with a gauge factor of ≈8350 at 50% strain (**Figure 6**a).[119] Significantly, the temperature sensor is not influenced by the external pressure stimulus and vice versa. Inspired by the human skin with configuration of epidermis, dermis, and hypodermis, a sandwich-like sensing system is able to monitor signals of temperature, light, and pressure synchronously without mutual signal interference (Figure 6b).[120] To simplify the operation and integration, Zhu et al. developed a bimodal sensor composed of two sinuous platinum (Pt) ribbons on a flexible polyimide substrate rather than multiple layers adopted by the foregoing mentioned examples.[116] Thanks to the construction of the dual thermosensitive ribbons as well as the constant temperature difference feedback circuit, the bimodal device is capable of simultaneously and independently monitoring artery temperature and wrist pulse. Overall, satisfactory progress has been made in the aspect of incorporation of two or three sensors into one flexible device and monitor signals discriminably without the crosscoupling effect.

The further integration of multiple sensors, signal processing, and even power supply modules usually employs relatively thicker films (several hundred micrometers) as supporting matrices because of handling ease during the fabrication. On the other hand, to improve the reliability of the sensing and wearability, several groups have successfully prepared ultrathin films with the thickness of a few micrometers to make the wearable device more comfortable to wear over the skin.[122,123] The effect of film thickness on the output of strain or ECG sensors has been investigated.[124–126] In addition, a good adhesion is often pivotal between some flexible sensors and skin, so that an adhesion layer is mostly applied despite its unsuitability for long-time measurements owing to skin irritation. Recently, a multifunctional flexible healthcare patch is developed by integrating an efficient skin temperature sensor and a gel-less sticky ECG sensor (Figure 6c,d).[121] It is found the film thickness should be thinner to accurately measure the skin temperature and the optimization of material concentration of CNT, PEIE, as well as PDMS could yield a relatively reliable gel-less ECG sensor. The integrated sensor patch is attached to a subject's chest under conditions of standing up, sitting down, standing up, and running states (Figure 6e,f). A small difference of about 1 °C is observed for the skin temperature between the flexible temperature sensor and commercial IR sensor because of the film thickness, which should be overcome in future to realize practical applications of wearable healthcare patches.

Simultaneous monitoring of chemical contents and physical properties is of high value to obtain complementary parameters, allowing to predict and diagnose adverse health conditions. For instance, it is probable to forecast dehydration during exercise through measuring pH level concurrently in sweat and skin temperature.[127] Several work has been demonstrated to monitor chemical states and physical conditions.[69,128,129] Recently, an ion-sensitive field-effect transistor (ISFET)-based pH sensor is incorporated with a printed temperature sensor, which is able to both measure skin temperature and compensate for the temperature effect of the ISFET (Figure 6g).[114] The advantage of employing the ISFET is attributed to its relatively simple direct current detection, while the conventional cyclic voltammetry (CV) method requires more complex measurements. The ISFET is constructed with InGaZnO thin-film, Al_2O_3, and

© 2019 WILEY-VCH Verlag GmbH & Co. KGaA, Weinheim

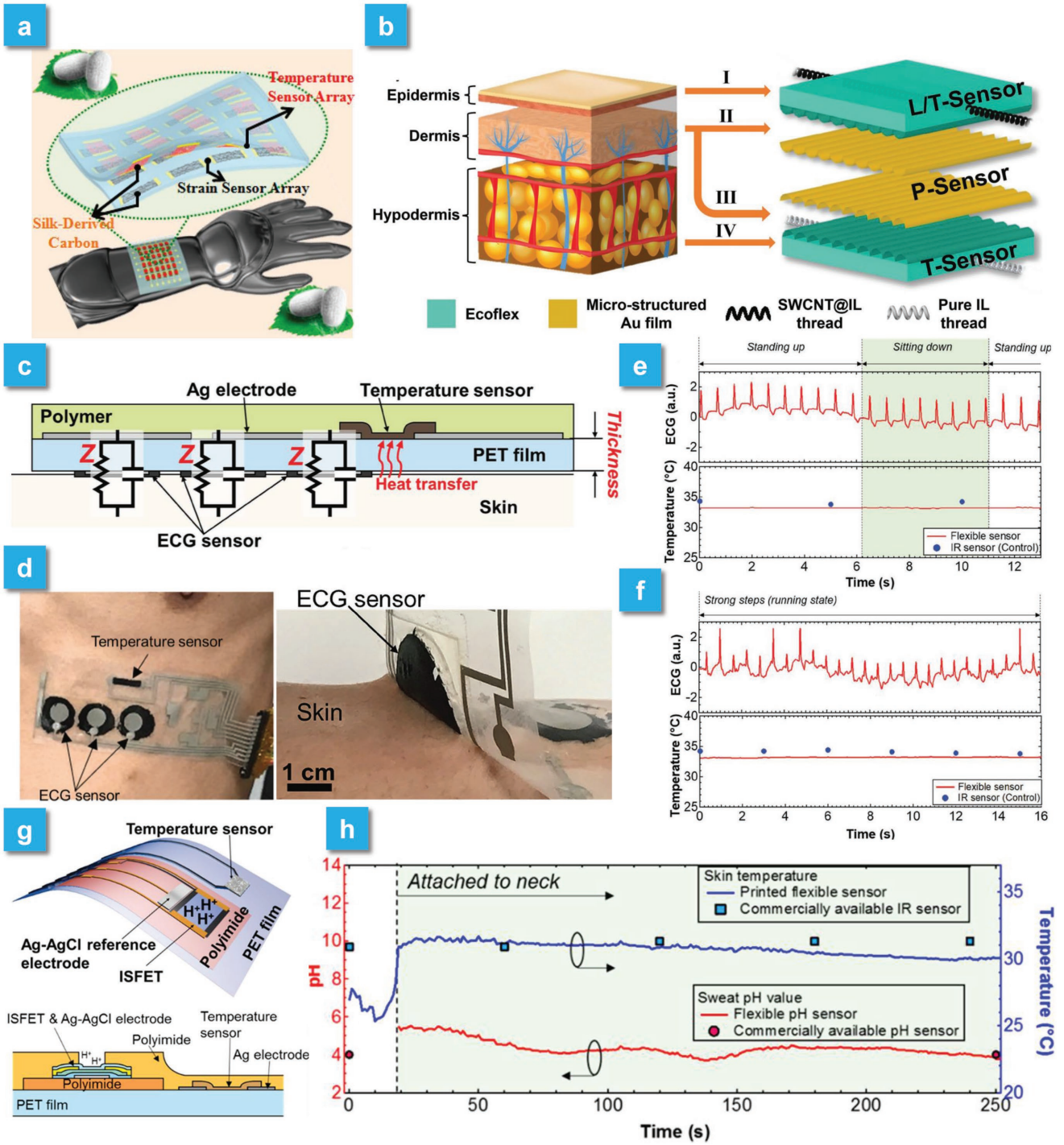


Figure 6. a) Schematic illustration of the silk-based combo temperature–pressure E-skin sensor. Reproduced with permission.[119] Copyright 2017, American Chemical Society. b) Schematic comparison of layered structure between human skin and SIMPS. I, Epidermis corresponds to light/temperature sensor; II, Dermis corresponds to pressure sensor; III–IV, Hypodermis corresponds to Temperature sensor and thermal insulating layer. Reproduced with permission.[120] Copyright 2017, John Wiley & Sons. c) Schematic image of the equivalent circuit of the ECG sensor and heat transfer through a PET film from skin to the device. d) Photographs of the fabricated device (left) and the adhesion test of the device peeled from skin (right). Results of the real-time ECG signal and skin temperature monitoring with a control temperature measurement using an IR sensor at e) standing up and sitting down states and f) strong-step states. c–f) Reproduced with permission.[121] Copyright 2017, John Wiley & Sons. g) Schematic of a wearable device integrating flexible pH and temperature sensors (top) and cross-sectional diagram of the device (bottom). h) Real-time pH and skin temperature acquired by the device. g,h) Reproduced with permission.[114] Copyright 2017, American Chemical Society.

© 2019 WILEY-VCH Verlag GmbH & Co. KGaA, Weinheim

a pH sensing membrane. It is found that when performing the measurement of pH level and temperature simultaneously based on the designed integrated flexible sensors, it is capable of compensating for the potential shift because of pH and temperature, giving rise to the precise pH monitoring over a wide temperature range. After attaching the wearable sweat ISFET-based pH sensor system onto a subject's neck by a double-side tape, the real-time monitoring of sweat pH and skin temperature comes true after exercising. The skin temperature is measured to be in the range of 30.0–31.7 °C with the pH at around 4.0, which agrees well with the control experiments (Figure 6h). However, the ISFET in this work cannot distinguish different chemicals, such as urea or lactic acid, as they also vary the pH values. Chemical sensitive membrane could be formed on the ISFET for selectively monitoring different molecules.

Due to complex fabrication procedures as well as diverse materials' requirement for different sensors, it is still challenging to integrate more than three sensors into a flexible chip, and meanwhile endowed with high mechanical flexibility, superior signal selectivity as well as excellent wearing comfort, although very limited reports have demonstrated this capability.[12,16,25,130] Undoubtedly, the incorporation of a plurality of sensors enables the E-skin with more intriguing functionalities.[131] For instance, the monitoring of heartbeat, skin temperature, ECG, etc. is traditionally conducted under subjects' resting state, which, as a matter of fact, cannot completely reflect bodies' health conditions. In view of this issue, Takei et al. demonstrated a multifunctional wearable health care monitoring device through integrating three sensors, including a skin temperature sensor, an ECG sensor, and an environmental ultraviolet (UV) light sensor, with a printed three-axis acceleration sensor (**Figure 7**a–c).[18] Considering the device required to be directly contacted with the skin, this multipurpose device is designed with a modular design comprising two detachable components (disposable and nondisposable layers) to address cost and hygiene concerns (Figure 7d). To be specific, a disposable sensor sheet that is directly worn on the skin takes into account cost-effective fabrication methods, low-cost materials as well as hygiene issues, whereas the other nondisposable or reusable sheet contains relatively expensive components. Both sheets are connected via a eutectic gallium–indium (EGaIn) liquid metal contact, which shows high stability under mechanical bending. By wearing the device onto the chest, simultaneously real-time monitoring of various sets of health information, including skin temperature, ECG, UV exposure, is realized under different physical activities, such as rest, fast steps, walking-pace steps and lying down (Figure 7e,f). It is found that the differences between running states and walking steps could be distinguished by observing the frequency and amplitude extracted from the acceleration sensor, indicating its role to differentiate health status at different physical conditions. Additionally, the stronger relationship between the trend of human motion and health states could be further analyzed by the approach of deep learning.

The incorporation of multiple sensors cannot only acquire comprehensive vital signs from human bodies, but also afford the ability to interact with environment. Zhu et al. recently demonstrated a multifunctional electronic skin endowed with multiple sensing abilities to perceive temperature and pressure stimuli, identify matter type and sense wind.[17] The introduction of various platinum ribbons array allows the formation of multiple sensing units, indicating a simple integration route to realize effective human–machine interaction capabilities. Furthermore, to increase the stretchability of skin-like integrated sensor systems, a stretchable and conformable matrix network (SCMN) was developed, which is provided with fascinating capabilities to simultaneously detect temperature, strain, humidity, ultraviolet light, magnetic field, pressure as well as proximity with good selectivity and discrimination (**Figure 8**a–c).[16] Inspired by the human skin with a complex somatosensory architecture, a SCMN comprising 100 sensory nodes connected by meandering wires is achieved as a multifunctional sensing platform. Taking merit of the meandering structure, the SCMN can be adjusted to conform to the skin area, exhibiting tunable sensing range and large-area expandability. It is found that a 25-fold expansion of the sensing area could be realized ranging from 16 cm^{-2} (original coverage) to 400 cm^{-2} (expandable size). Additionally, owing to the insulation of polyimide dielectric thin films, 3D integration could be achieved by sharing a sensory node with different functional sensors. Via coupling the SCMN configuration with a prosthetic hand, the temperature could be accurately estimated by the intelligent hand when performing grasp/release manipulations (Figure 8d–f). Such skin-inspired SCMN with considerable merits could be applied to diverse fields, such as humanoid robotics, new prosthetics as well as health-monitoring.

In the previous section, various types of chemical sensors and their recent developments are illustrated. However, the general reported noninvasive biosensors can only detect a single analyte or biofluid at a time. Recently, Kim et al. developed a dual epidermal biofluid sampling and analysis strategy, allowing the simultaneous detection of sweat at an anode and interstitial fluid at a cathode.[117] Due to the complex compositions of biofluid such as sweat, it is still challenging to detect a plurality of biomarkers using a single wearable device and perform real-time signal processing to accurately evaluate health status. Remarkably, Gao et al. demonstrated a wearable flexible integrated sensing array (FISA) for multiplexed in situ perspiration analysis, which realizes simultaneous and selective measurement of abundant sweat biomarkers and skin temperature (Figure 8g–i).[25] At an unprecedented level of integration, this work merged various functionalities, including signal transduction, conditioning, processing as well as wireless transmission, into a single flexible system for real-time monitoring of subjects' physiological states, which comprises skin-interfaced plastic sensors (five different sensors) and silicon integrated circuits consolidated on a flexible board (more than ten chips). By wearing the FISA on different parts of the body, such as wrists, arms, or forehead, the mechanically flexible wearable sensor can be applied for prolonged indoor and outdoor activities, allowing the real-time assessment of health status (Figure 8j). In spite of five sensors synchronously performing system-level measurements, excellent selectivity is maintained upon varying each analyte's concentration (Figure 8k). In addition, the incorporated temperature sensor assists in eliminating the effect of temperature variation in the readings. It is found the potentiometric sensors are hardly influenced by the temperature, but the responses of glucose and lactate sensors rise quickly with increasing the solution temperature from 22 to 40 °C, indicating the effect of

© 2019 WILEY-VCH Verlag GmbH & Co. KGaA, Weinheim

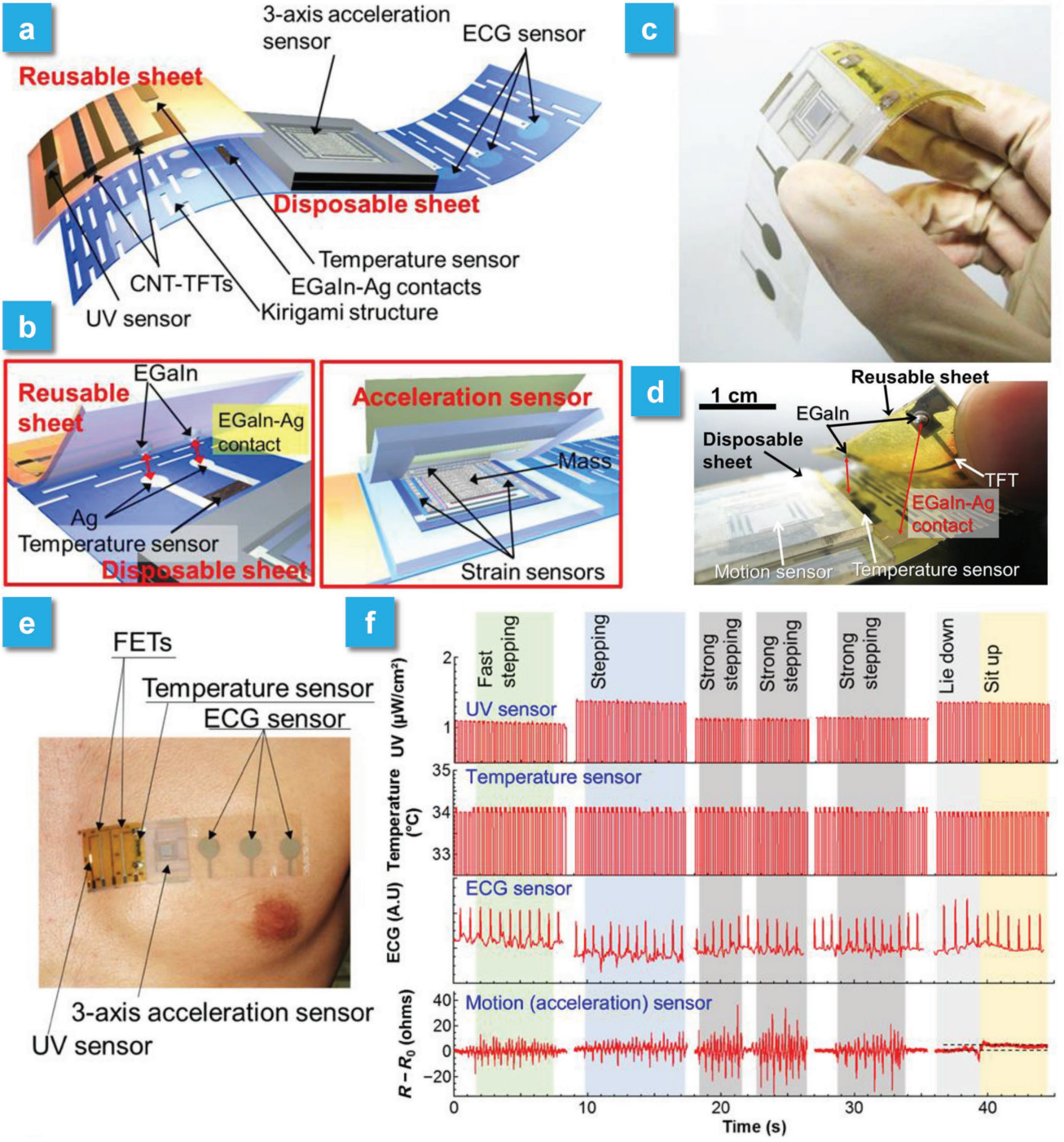


Figure 7. Schematics of a) the whole device structure, including both disposable and reusable components, b) EGaIn and Ag contact region between the sheets (left) and three-axis acceleration sensor (right). c) Image of the fabricated device. d) Image of the device, particularly focused on the EGaIn-Ag contact region between the sheets. e) Image of the multifunctional device attached directly onto the skin. f) Real-time acceleration (motion), ECG, skin temperature, and UV monitoring results. All panels reproduced with permission.[18] Copyright 2016, American Association for the Advancement of Science.

enhanced enzymatic performance, the readings of which can be compensated by temperature variations (Figure 8l). It is envisioned that large database could be established through community participation to drive forward the data-mining techniques, allowing the better comprehending of health conditions.

3.2. Self-Healing Material-Based Devices

To improve the reliability, extend the lifespan as well as further increase the functionality, such as ultrahigh stretchability without performance degradation for skin-interfaced sensors,

© 2019 WILEY-VCH Verlag GmbH & Co. KGaA, Weinheim

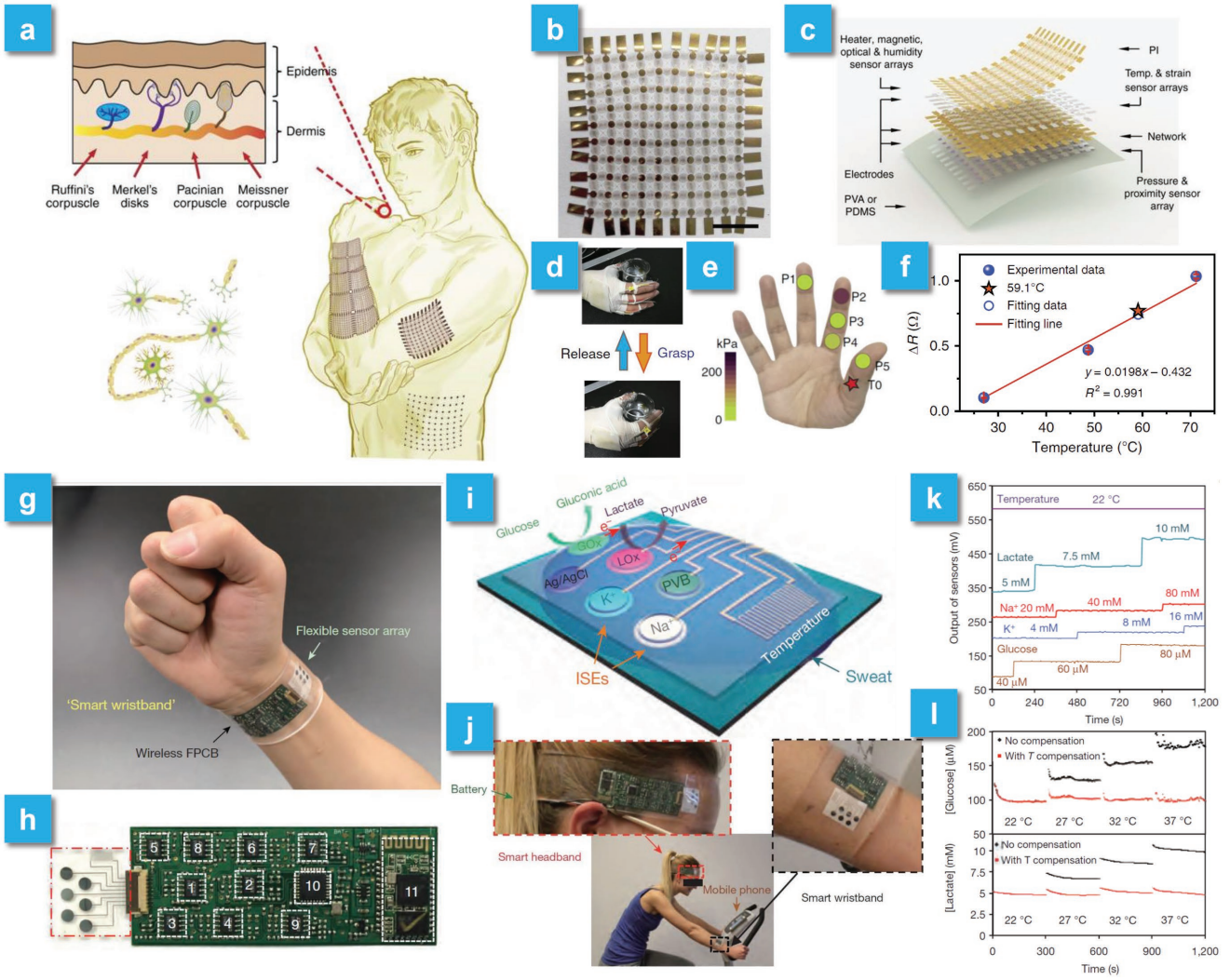


Figure 8. a) Schematic illustration of SCMNs conforming to the surface of a human arm and an expanded network (expansion: 200%) conforming to the surface of a human abdomen (right); the tree branch-like connections of neurons (left bottom); the sensory receptors of the glabrous skin (left top). b) Optical image of the fabricated polyimide network. c) Schematic layout of an SCMN—an integrated sensor array with eight functions. (temp.: temperature). d) Images show operations of the intelligent prosthetic hand to grasp (upper) and release (bottom). e) Pressure distribution contour on the fingers when the intelligent prosthetic hand is grasping a water cup and sensing temperature of 59.1 °C. f) Temperature estimation by the fitting equation when the intelligent prosthetic hand is grasping. a–f) Reproduced with permission.[16] Copyright 2018, Nature Publishing Group. g) Photograph of a wearable FISA on a subject's wrist, integrating the multiplexed sweat sensor array and the wireless FPCB. h) Photograph of a flattened FISA. i) Schematic of the sensor array for multiplexed perspiration analysis. j) Photographs of a subject wearing a "smart headband" and a "smart wristband" during stationary cycling. k) System-level interference studies of the sensor array. l) System-level real-time temperature *T* compensation for the glucose and lactate sensors. g–l) Reproduced with permission.[25] Copyright 2018, Nature Publishing Group.

the flexible electronic devices are envisaged to gain attractive self-healing capability via mimicking the natural systems. Typically, the self-healing systems can be classified into extrinsic and intrinsic self-healing. The extrinsic self-healing requires external triggers (e.g., heat, light, or chemicals) to initiate the self-healing processes upon damage. These external healing agents are usually encapsulated in capsules or vascular network. The capsule-based healing system is implemented via directly spreading capsules into a matrix, but after a single damage event, it suffers from local function depletion.[132] To overcome this issue, the vascular self-healing systems are developed through sequestering healing agents in networks in the form of capillaries or hollow channels. However, their complicated fabrication processes are not appropriate for practical applications.[19] Another promising strategy to realize self-healing systems is constructed from intrinsic self-healing materials, requiring no external healing agents. Most of such self-healing materials are dominated by covalent or noncovalent self-healing mechanisms based on dynamic reversible bond interactions, such as hydrogen bonding, π–π stacking, dipole–dipole or van der Waal's interactions, which spontaneously takes place at ambient circumstances to recover the functionality upon damage.[133]

Regarding to E-skin applications, it is greatly crucial to endow self-healing materials with the capability to restore not only mechanical features, but also high electronic conductivity,

© 2019 WILEY-VCH Verlag GmbH & Co. KGaA, Weinheim

although it is a formidable challenge due to the difficulty in achieving high bulk electrically conductive self-healing materials. One probable route is to develop conductive polymers through rationally introducing reversible bonds within polymeric matrix.[134,135] For instance, Yu et al. demonstrated a hybrid gel system, where a 3D nanostructured polypyrrole (PPy) gel contributes to conductivity and metal–ligand supramolecules mainly serve as self-healing without any external stimuli.[135] A relatively high conductivity of 0.12 S cm^{-1} is achieved compared to its congeners. Another facile way to obtain conductively self-healable systems relies on directly depositing conductive materials onto the surfaces of nonconductive self-healing substrates.[136,137] The healing process enables the separated conductive layers into contact. Nevertheless, the conductive layers may suffer from exfoliation from the substrates after repeated deformation, limiting their long-term stability for practical applications. To achieve more reliable self-healing systems with higher conductivities as well as better mechanical stability, a promising strategy is to merge conducting fillers into nonconductive self-healing matrices, allowing the formation of conductive self-healing composites. Until now, a number of materials have been employed to serve as conducting fillers, such as metallic nanowires,[138] graphene based materials,[139] CNTs,[140–142] metal particles,[143] liquid metal,[27] or ionic liquid[144] for the sake of improving performance of the self-healing material-based devices. A pioneering work is made by Tee et al. via incorporating micronickel (μNi) particles into a supramolecular polymeric hydrogen-bonding network.[145] The high electrical conductivity of 40 S cm^{-1} is gained with good stretchability and ≈90% of its initial conductivity is able to be recovered after healing duration of 15 s.

With these performance-enhanced flexible conductive self-healing materials as building blocks, diverse flexible sensors have been developed provided with superior self-healing capabilities.[19,134,146,147] A recent impressive work was conducted by Lee and co-workers.[140] Through incorporating CNTs, graphene, or silver nanowires into borax/polyvinylalcohol-based self-healing nanomaterials, the self-healable strain sensor is capable of withstanding strain up to 1000% with a high gauge factor of 1.51, partially attributed to rapid electrical healing speed (within 3.2 s) as well as self-healing efficiency (98 ± 0.8%). There is no significant variation observed after stretching the flexible sensor to 700% for 1000 cycles. Darabi et al. demonstrated a stretchable and self-healable wireless human motion detector based on the matrices of autonomous intrinsic self-healing of physically and chemically crosslinked polymers, which can collect the human physiological information of respiratory, pulse, and muscle motions.[28] The introduction of a covalent crosslinking between poly(acrylic acid) and *N,N″*-methylenebis-acrylamide enhances the mechanical performance of the hydrogel. Such a double network hydrogel presents 100% mechanical recovery in 2 min with distinct ultrastretchability of 1500%. Although tremendous progress has been made in the self-healable materials/devices, the integration of a multifunctional electronic system based on self-healing materials has not been realized, which is primarily due to the challenges of different sophisticated needs to fabricate each component and in the lack of massive integration of individual self-healable modules into a system.

To address these issues, a pioneering work has been carried out by Bao et al., realizing a multifunctional stretchable and self-healable electronic skin system (MSES) (**Figure 9**).[26] This is innovatively achieved via applying a self-healing polymer matrix surrounding a nanowire conductive network. Upon broken, the conductive network is able to reconstruct itself dynamically and autonomously heal to recover both high conductivity and mechanical properties. The backbone materials of self-healing polymer matrix (PDMS-$MPU_{0.4}$-$IU_{0.6}$) are composed of strong (4,4′-methylenebis (phenyl urea) unit, MPU), weak (isophorone bisurea unit, IU) dynamic bonding units, and poly(dimethylsiloxane) (PDMS), showing a high stretchability up to 1600% strain and a high fracture toughness of (12 000 J m^{-2}). Such a crosslinked network PDMS-$MPU_{0.4}$-$IU_{0.6}$ is then coupled with elastic carbon nanotubes (CNTs), allowing the formation of conductive and self-healable nanonetwork. The self-healing process of the electrode is categorized into two processes, including spontaneous physical contact after the mechanical damage inflicted on it and reorganization of the CNT network during restructuring of the polymer matrix (Figure 9a). Relying on the designed materials as well as facile bonding fabrication process, the MSES platform is demonstrated for the first time through the integration of a strain monitor, an ECG sensor and a light-emitting capacitor (LEC) array (Figure 9b). These electronic modules are self-bonded onto the PDMS-$MPU_{0.4}$-$IU_{0.6}$ substrate. Owing to its low modulus and high stretchability, the MSES could be seamlessly mounted onto the human skin for continuous healthcare monitoring. The physiological information is able to be recorded by the sensors, processed and subsequently transmitted wirelessly to the self-healable LEC display for visual interpretation (Figure 9c). Such system-level multifunctional self-healable E-skins afford intriguing potentials for future robust and unbreakable wearable electronics.

3.3. Self-Powered Flexible Sensors

To successfully manipulate a wearable multimodal system sustainably and independently, the power module plays a highly significant role in efficient signals' generation, transmission, and processing. Indeed, the development of flexible supercapacitors or batteries serves as a promising strategy to conform to the mainstream of wearable electronics. However, such flexible energy-storage devices are limited by relatively low energy and power densities, hindering their practical applications, especially in remote regions. Fortunately, the burgeoning self-powered systems are emerged as alternative energy-harvesting techniques, which are envisioned to substitute for the traditional bulky power components. The self-powered sensors are capable of implementing the functions by themselves sustainably and independently without external power sources through transforming the ubiquitous energy from ambient or human bodies, primarily including mechanical energy, thermal energy as well as solar energy. A great deal of efforts in the past decade have thus been dedicated to improving the energy conversion efficiency, flexibility, or conformability of the self-powered systems via judiciously constructing new materials or structures.[148,149]

© 2019 WILEY-VCH Verlag GmbH & Co. KGaA, Weinheim

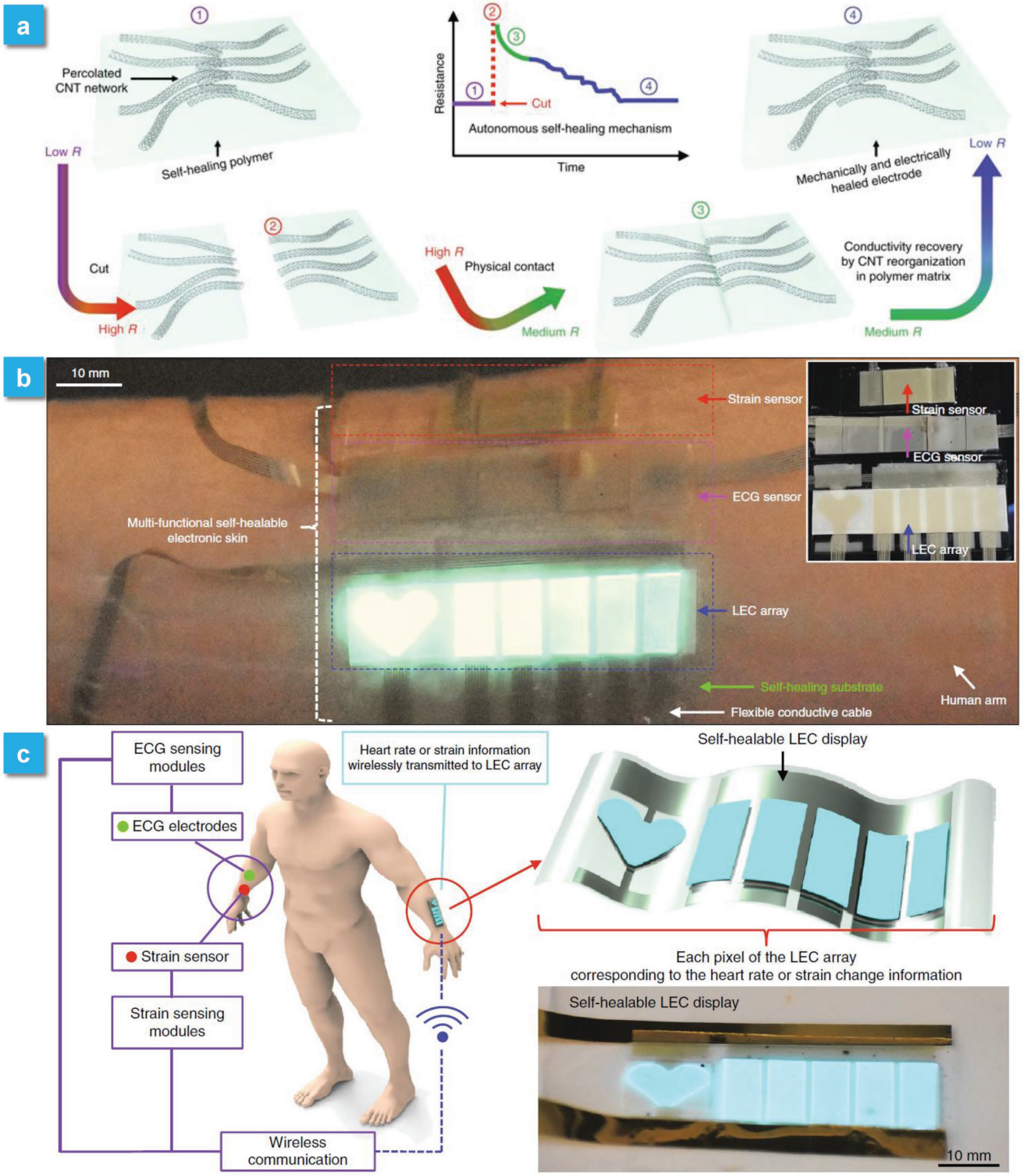


Figure 9. a) Proposed recovery mechanism for CNTs embedded in self-healing polymer matrix. CNT network reconstruction is based on observations as follows: (1)) continuous reduction of resistance over time, (2)) recovery of stretchability, 3) maintaining high conductivity with strain for recovered electrode, 4) lack of clear physical separation in the CNT network in the recovered cut region. b) Multifunctional self-healable electronic skin device on skin while performing LEC operation, which emits a blue-green light. Inset: electronic skin on rigid substrate. c) Overview of the system with sensors wirelessly communicating values to the display. All panels reproduced with permission.[26] Copyright 2018, Nature Publishing Group.

© 2019 WILEY-VCH Verlag GmbH & Co. KGaA, Weinheim

Mechanical energy is mostly derived from the movement of human bodies or ambient vibrations. Typically, triboelectric and piezoelectric effects are two reliable approaches to convert mechanical energy to electricity for wearable electronics. Since the first report of flexible triboelectric nanogenerators (TENGs) by Fan et al.,[150] several groups have been involved in applying TENGs on skin-inspired sensors, targeting at the realization of battery-free monitoring and diagnostic systems.[111,151–157] For instance, Pu et al. reported a mechnosensational TENG (msTENG)-based noninvasive micromotion sensor that is capable of translating eye blink into control command based on a multifilm structure, which could be flexibly mounted behind an eyeglass arm (**Figure 10**a).[158] Owing to its high sensitivity (≈750 mV), the smart sensor can not only control the household appliances, but also exhibits the promising functionality as a hands-free typing system (typing with eye blinking), making life easier and more fascinating (Figure 10b). To monitor heart-rate in real time, Lin et al. demonstrated a self-powered wireless body sensor network (BSN), comprising a downy-structure-based TENG (D-TENG), a power management circuit, a heart-rate sensor, a signal processing module as well as a Bluetooth module.[159] Under natural human walking, a power as high as 2.28 mW with conversion efficiency of 57.9% is achieved from the wearable D-TENG, which provides essential electricity for the BSN configuration. The majority of current self-powered TENG devices typically aim at a single category of human activities due to their incapability in response to various mechanical stimuli and limitation in sensing range. Ho et al. reported a stretchable TENG based on a coaxial core-sheath fiber.[152] Taking advantage of the unique combination of materials engineering and configuration design, such fiber TENGs are capable of responding to various human activities, including finger bending, walking, forearm rotation, pulse, respiration, and throat-related activities. Additionally, the traditional TENGs usually require vertical contact-separation mode with a macroscale air gap, otherwise the device may suffer from the performance degradation. However, the human-interactive applications demand the flexible sensors to be conformally attached onto fingers or elbow joints, where the macroscale separation mode is hard to realize. Fortunately, microfluidic-based TENGs could resolve this issue via filling liquid into the chamber.[160] The generation of output signals depends on the different volumes of liquid flowing within the channel, making it possible to synchronously measure both the magnitude and frequency of pressure. However, there exist intrinsic limitations of wearable triboelectric E-skin, such as high variations of triboelectric signals in humid ambient, weak power generation due to mechanical damage by friction and relatively complex structure architectures.[111] Piezoelectric materials-based E-skin sensor is able to overcome the foregoing issues. Recently, Lee's group developed a self-powered flexible piezoelectric pulse sensor using an inorganic-based laser lift-off technique with $Pb[Zr_x,Ti_{1-x}]O_3$ (PZT) film as the building block to monitor health in real time (Figure 10c).[161] The flexible piezoelectric sensor shows a sensitivity of 0.018 kPa^{-1} with response duration of 60 ms, which could respond to lower frequency vibrations

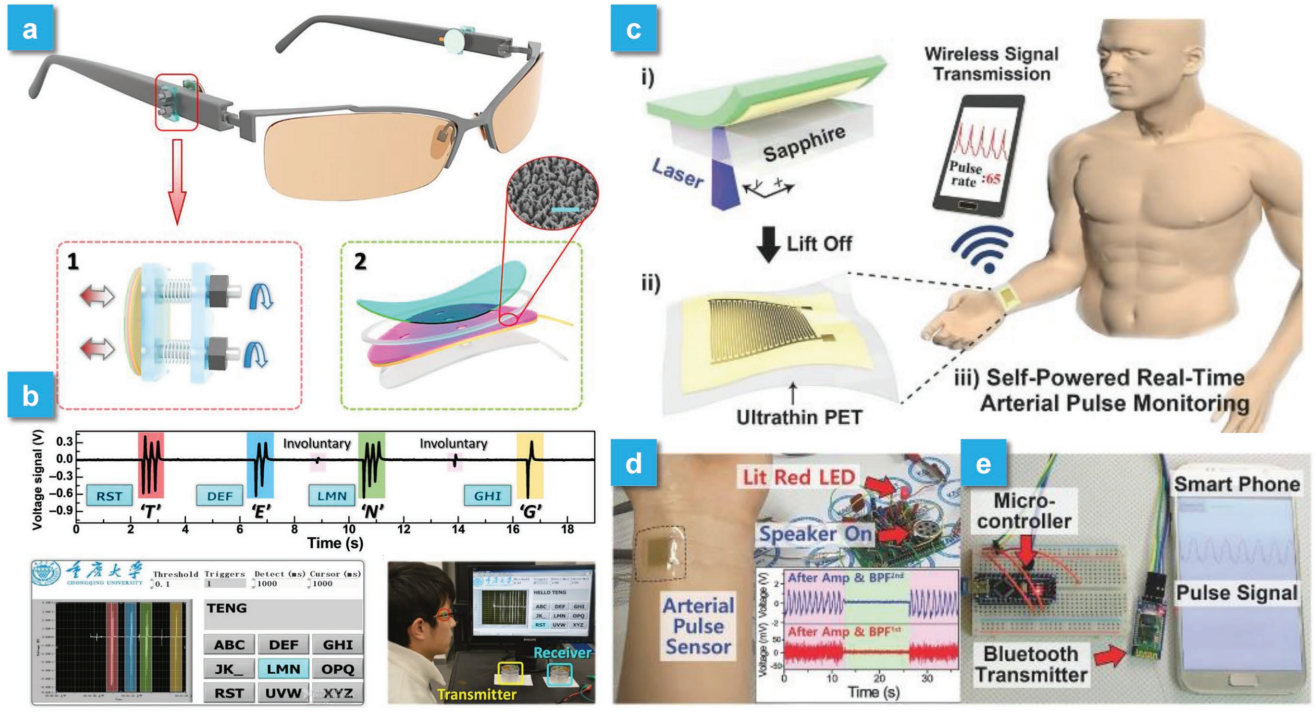


Figure 10. a) Schematic structure of a pair of ordinary glasses mounted with msTENG. b) Correspondence between signals and letters typed in the demonstration of a hands-free typing system with adjustable threshold, detecting time, and cursor shift interval, and demonstration of the msTENG-based hands-free wireless typing system. a,b) Reproduced with permission.[158] Copyright 2017, American Association for the Advancement of Science. c) Schematic illustration of the fabrication process for self-powered pressure sensor. d) Photograph of the LED and speaker unit operated synchronously corresponding to the radial artery pulse. e) Photograph of wireless transmission of the pulse to a smart phone, showing capability for a real-time arterial pulse monitoring system. c–e) Reproduced with permission.[161] Copyright 2017, John Wiley & Sons.

© 2019 WILEY-VCH Verlag GmbH & Co. KGaA, Weinheim

from 0.2 to 5.0 Hz and higher frequency sound waves of 240 Hz. More importantly, the pulse signals can be wirelessly transmitted to a smart phone (Figure 10d,e).

Thermal energy is quite common in our surroundings and particularly, waste heat energy abundantly exists in industries, combustion engines, solar heat, human bodies, etc. The dexterous reclamation of these low-grade heat is envisaged to realize a decarbonized ecosystem through smart energy conversion technologies. Undoubtedly, if the wearable integrated skin-interactive systems are endowed with the capability to efficiently convert these ample waste heat to electricity, it is conceivable to not only drive a couple of sensors without external bulky power supply, but also fulfill an environmentally friendly community. With this motivation in mind, several groups have been dedicated to scavenging energy for sensing principally on the basis of thermoelectric or pyroelectric effect. Thermoelectric generators, chiefly constructed with solid-state semiconductors materials, rely on the conversion of thermal energy into electricity via Seebeck effect demanding spatial temperature gradient. To boost the output power of thermoelectric generators, although, as an alternatively promising strategy, thermocells have been applied to harvest waste heat based on electrons transfer between redox couples and electrodes due to the nature of relatively high Seebeck coefficient, such steady temperature variations are scarce in natural surroundings.[162–164] On the contrary, pyroelectric generators (PyNGs) are subjected to time dependent temperature fluctuation so as to trigger the energy conversion processes.[165–169] For example, the temperature of body exhaled gas is similar to human body, which is generally higher than the environmental temperature, especially in winter. As such, a wearable self-powered breathing sensor is developed via integrating a PyNG configuration on a respirator.[170] At 5 °C ambient temperature, the PyNG can not only generate high enough power to drive liquid crystal display or LEDs, but also function as a respiration sensor to monitor the frequency and intensity of breathing pertaining to the symptoms of human body.

To further improve the scavenging efficiency of low grade heat, supplementary power generators are rationally hybridized to concurrently harvest energy.[166,171–173] Because of the dual nature of ferroelectric poly(vinylidene fluoride) (PVDF) with both piezoelectric and thermal properties, a self-powered piezoelectric–pyroelectric nanogenerator is demonstrated built from nonwoven nanofiber membranes via facile electrospinning methods.[174] Through the coupling of piezoelectric and pyroelectric effects, the total output signal could be enhanced with the synergistic current expressed as[175]

$$I_{\text{piezo+pyro}} = \frac{d_{33} A \mathrm{d}\sigma}{\mathrm{d}t} + \frac{pA\mathrm{d}T}{\mathrm{d}t} \tag{2}$$

where d_{33}, A, $\mathrm{d}\sigma/\mathrm{d}t$, p, and $\mathrm{d}T/\mathrm{d}t$ are the piezoelectric coefficient, effective area of the device, the rate of mechanical stress change, pyroelectric coefficient, and the rate of temperature change, respectively. The generation of hybrid piezoelectric–pyroelectric current is achieved by periodically turning the hot airflow, similar to the exhaust emissions of cars, on (bending and heating) and off (unbending and cooling). Furthermore, to minimize the energy loss during the friction, Zi et al. demonstrated a triboelectric–pyroelectric–piezoelectric hybrid cell consisting of a sliding mode TENG and pyroelectric–piezoelectric nanogenerator (PPENG).[172] Due to the capability of PPEGN to scavenge the friction-induced heat and mechanical energy, such hybrid cells present about two-fold performance of charging a super capacitor higher than that of the TENG alone, which pushes forward the potential applications in multifunctional self-powered sensors. Although tremendous progress has been made in harvesting waste heat, formidable challenges still exist in autonomously continuous extraction and utilization of the low-grade thermal energy. To surmount this obstacle, a self-governing thermo-mechano-electrical system (TMES) has been recently demonstrated by Ho and co-workers.[166] Because of structural instability induced by thermal responsive bending shape and air-solid temperature gradient, the TMES can simultaneously harvest self-created temperature fluctuations and mechanical mobility, allowing the self-propelled multimodal locomotions, which in turn promote the self-sustained temperature fluctuations to achieve perpetual movement for ceaseless power generation (**Figure 11**a–d).

Solar energy is another rich source, usually relying on photovoltaic cells to convert sunlight into electricity.[176,177] However, there are several intrinsic limitations, such as uncertain of climate or failure to connect sensors with the solar cells. In view of these issues, Yun et al. demonstrated a stretchable array of micro-supercapacitors (MSCs), which are charged by commercial Si-based solar cells (SCs) to drive an integrated strain sensor.[29] The MSCs could maintain 80% of their original capacitance after 5 000 charge/discharge cycles. Furthermore, no significant change is observed after 1000 biaxial stretching/releasing cycles by 30%. Through using the electricity stored in the MSCs from the SCs, the integrated system is able to be wrapped onto the wrist to successfully monitor external strain as well as arterial pulse. However, the traditional Si-based SCs are typically brittle and their thicknesses are several hundreds of micrometers, decreasing the compatibility in wearable applications. As an intriguing alternative, organic photovoltaics could also provide self-powered functionality to be adhered onto skin and complex biological tissues. However, because of the unsteady output power under mechanical deformation, the ultraflexible organic power sources have not been integrated with the sensors until a recent unprecedented work by Someya et al.[30] On a 1 μm thick ultraflexible substrate, organic electrochemical transistors (OECTs) coupled with organic photovoltaic power sources are fabricated, rendering the measurement of biometric signals with a high signal-to-noise ratio up to 40.02 decibels to record cardiac signals (Figure 11e,f). The formation of nanograting structures at a periodicity of 760 nm prominently boosts the efficiency of organophotovoltaics, making the cells' efficiency insensitive to the angle of incident light and thus giving rise to a power-conversion efficiency of 10.5%. Due to its superior skin-conformability, the self-powered OECT sensor could be adhered onto the fingertip to record cardiac signals driven by light-emitting diodes. The sensitivity is around three times higher than that of OECTs powered by external electrical sources (Figure 11g–i).[178] The superior mechanical flexibility and biocompatibility of the ultrathin device (several micrometers) enables it to be seamlessly attached onto an exposed rat heart for in vivo recording ECG signals (Figure 11j–k).

© 2019 WILEY-VCH Verlag GmbH & Co. KGaA, Weinheim

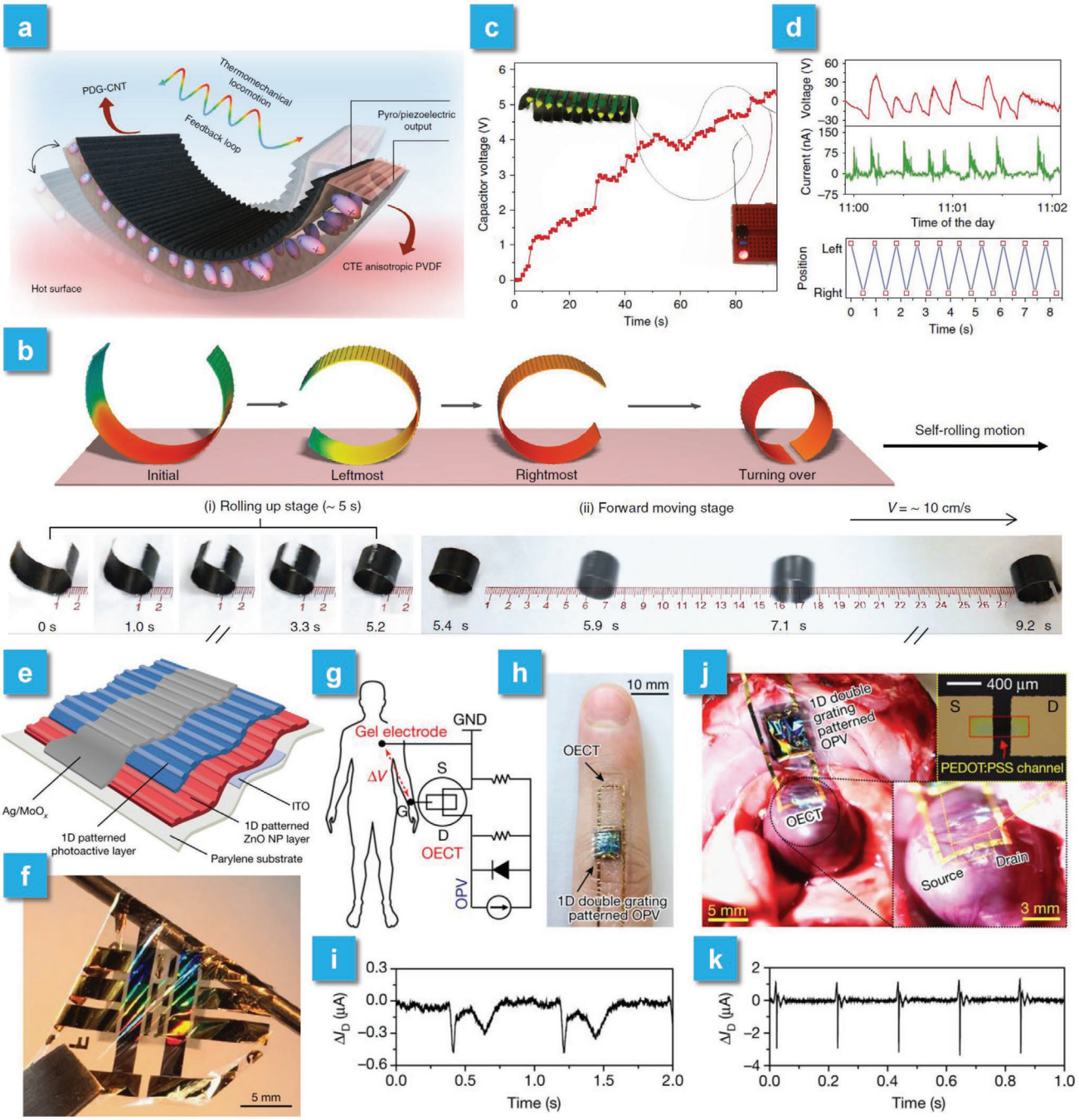


Figure 11. a) Schematic illustration of the design concept of thermo-mechano-electrical conversion based on a bimorph actuator. b) Schematic representation and snapshots of a self-rolling motion of TMES. c) Charging characteristic of TMES-bot and an inset photograph of a lighted LED using a charged capacitor. d) Open circuit voltage/short circuit current generated by locomotion of TMES under an ambient outdoor environment (top) and photothermal-directed cyclic oscillations of the TMES (bottom). a–d) Reproduced with permission.[166] Copyright 2018, Nature Publishing Group. e) Structure of the OPV device. f) Photograph of the OPV device wrapped over a spatula rod and pulled by tweezers. g) Wiring diagram for cardiac signal recording. h) Photograph of the self-powered integrated electronic device attached to a finger. i) Measured output current from the recorded cardiac signal trace, under light illumination. j) Photograph of the self-powered integrated electronic device attached to the heart of a rat. k) Measured output current from the ECG trace, under light illumination. e–k) Reproduced with permission.[30] Copyright 2018, Nature Publishing Group.

4. Large-Scale Flexible Devices

As the core of booming IoTs, the multifunctional wearable electronics/devices are envisioned to be realized over large scales on the order of square centimeters to square meters, so that the mechanically flexible network could be conformally wrapped onto arbitrary surfaces to quantify various stimuli, while a single-pixel circuitry cannot implement this goal. Since the first

© 2019 WILEY-VCH Verlag GmbH & Co. KGaA, Weinheim

demonstration of integrated flexible pressure sensor matrix,[179] several groups have been devoted to constructing high-performance macroscale flexible systems to realize objects' spatial and temporal profile mapping based on temperature or pressure sensors array.[3,22,23,63,180,181] Representative work in terms of such macroscale artificial skin is demonstrated by Javey and co-workers.[22,23] With the backbone of semiconductor nanowires (NWs), a large-area active-matrix backplane (7×7 cm^2) is performed to monitor applied pressure profiles comprising a flexible pressure-sensor array (18×19 pixels) at a low operating voltage (<5 V) (**Figure 12**a–c).[22] Furthermore, in order to attain an instantaneous visual response without complex data acquisition, organic light-emitting diodes (OLEDs) components are merged into the flexible sensor matrix, working as a user-friendly display in response to the external pressure.[23] Although tremendous progress has been made regarding the aforementioned macroscale flexible devices, the pixel yield and resolution could be further improved for elaborate mapping. On the other hand, the cost should be considered if the versatile human-interactive devices target at penetrating into common households for daily use.

Recently, printing technologies (e.g., inkjet, roll-to-roll, gravure printing, etc.) have attracted widespread research attentions in constructing large area flexible devices because of their cost-effect characteristics and rapid manufacturing procedures.[21,184–189] For the detailed description of each printing methodology, such as principles or printable nanomaterials, interested readers may refer to the excellent reviews by Chen et al. and Wu et al.[190,191] This section will concentrate in presenting the latest advances regarding to skin-inspired systems realized by relatively facile efficient printing techniques. Compared to their counterparts (e.g., photolithography, electron-beam lithography, focused ion-beam lithography, etc.), the printing approach requires no complicated clean-room settings and expensive chemicals, while allows the manufacturing of functional devices at large scales. For instance, inspired by unique sensing functionality of animals, Takei et al. demonstrated artificial electronic whiskers (e-whisker) coupled with strain and temperature sensors array by fully printed methods (e.g., screen printing).[58] Taking advantage of the high sensitivity of strain and temperature sensors on the e-whisker, the 3D physical space and temperature distributions are obtained. Furthermore, via employing only a screen printing, a fingerprint-like structure is reported, which is capable of simultaneously monitoring three-axis forces based on tactile and slip forces detection as well as measuring temperature (Figure 12d–f).[182] Four strain sensors and one temperature sensor are merged into each pixel on a 8×8 cm^2 substrate (Figure 12e). Through the introduction of advanced commercially available printing facilities, high-resolution patterns as low as 10 μm are anticipated to be achieved over larger scales. Additionally, the flexible devices with the capability of mass production at low cost are particularly significant in single-use applications with disposable features. For example, roll-to-roll (R2R) gravure printed electrodes are recently demonstrated for various electrochemical sensing scenarios (Figure 12g).[21] The electrode arrays consist of working, reference, and counter electrodes in the formation of a canonical 3-electrode system, rendering the detection of ions, heavy metals, metabolites, etc. (Figure 12h). Different from the screen printing using the thickness of ink up to 100 μm, the relatively thin layer of ink (≈10 μm) for the R2R gravure approach leads to insufficient conductivity, thus a bilayer working electrode is applied with a silver ink layer to optimize the conductivity. Impressively, the scale of flexible substrates based on the R2R approach is up to 150 m, making the electrodes serve as disposable strips for point-of-care diagnostics, such as in situ sweat monitoring.

To enable the realization of mechanically exquisite and on-demand objects at fast speed, 3D printing is an excellent candidate, with the capability of incorporating conductive materials into microchannels to form integrated circuits and sensors.[28,64,183,192] Benefiting from such merits of 3D printing, Ota et al. developed 3D integrated electronic systems for a variety of sensing, actuation as well as signal processing operations through embedding liquid metal-based components and silicon integrated circuits (Figure 12i,j).[183] Particularly, a form-fitting glove tailored to patient's body is demonstrated by integrating a programmable heater and a temperature sensor for thermotherapy to boost blood flow and reduce pain at the point of injury (Figure 12k). Definitely, such multifunctional printable devices could be extended to other associated therapeutic and health diagnostics, such as wound healing or drug delivery. The scalable fabrication is attainable by packing more electronic modules.

5. Conclusions and Outlook

The past decade has witnessed enormous advances in skin-like wearable electronics from fundamental syntheses of innovative nanomaterials to demonstration of fascinating applications, such as healthcare monitoring, soft robotics, artificial intelligence, and human–machine interfaces. To reach the ultimately promising target of state-of-the-art flexible E-skin systems, scientists from diverse research fields have been involved in this booming subject. In this report, we have focused on the discussion of versatile wearable sensors endowed with intriguing "multifunctionalities," the trend to future wearable electronics. To start with, different categories of sensors are introduced accompanied with the key technical challenges. The multifunctional human-interactive flexible sensors are then highlighted, including multimodal sensor systems, self-healing material-based devices, and self-powered flexible sensors. Their latest progress is critically presented. Additionally, the development of large-scale flexible devices by rapid and cost-effective means is briefly demonstrated. Owing to the unique features of skin-inspired sensors, such as flexibility, stretchability, elasticity and biocompatibility, wearable sensors could be conformally and seamlessly attached onto the human body for the sensitive monitoring of vital signs and perception of abundant ambient information.

Despite the tremendous progress made in this burgeoning topic, challenges still exist for practical applications. For example, the measurement of flexible sensors in harsh environment, such as humid, rainy circumstances, low-temperature (below 0 °C) environment, and even outer space, is rarely studied. The artificial superhydrophobic coatings are a promising strategy to protect the flexible electronics, but they have been only applied to unitary devices.[193,194] The multifunctional

© 2019 WILEY-VCH Verlag GmbH & Co. KGaA, Weinheim

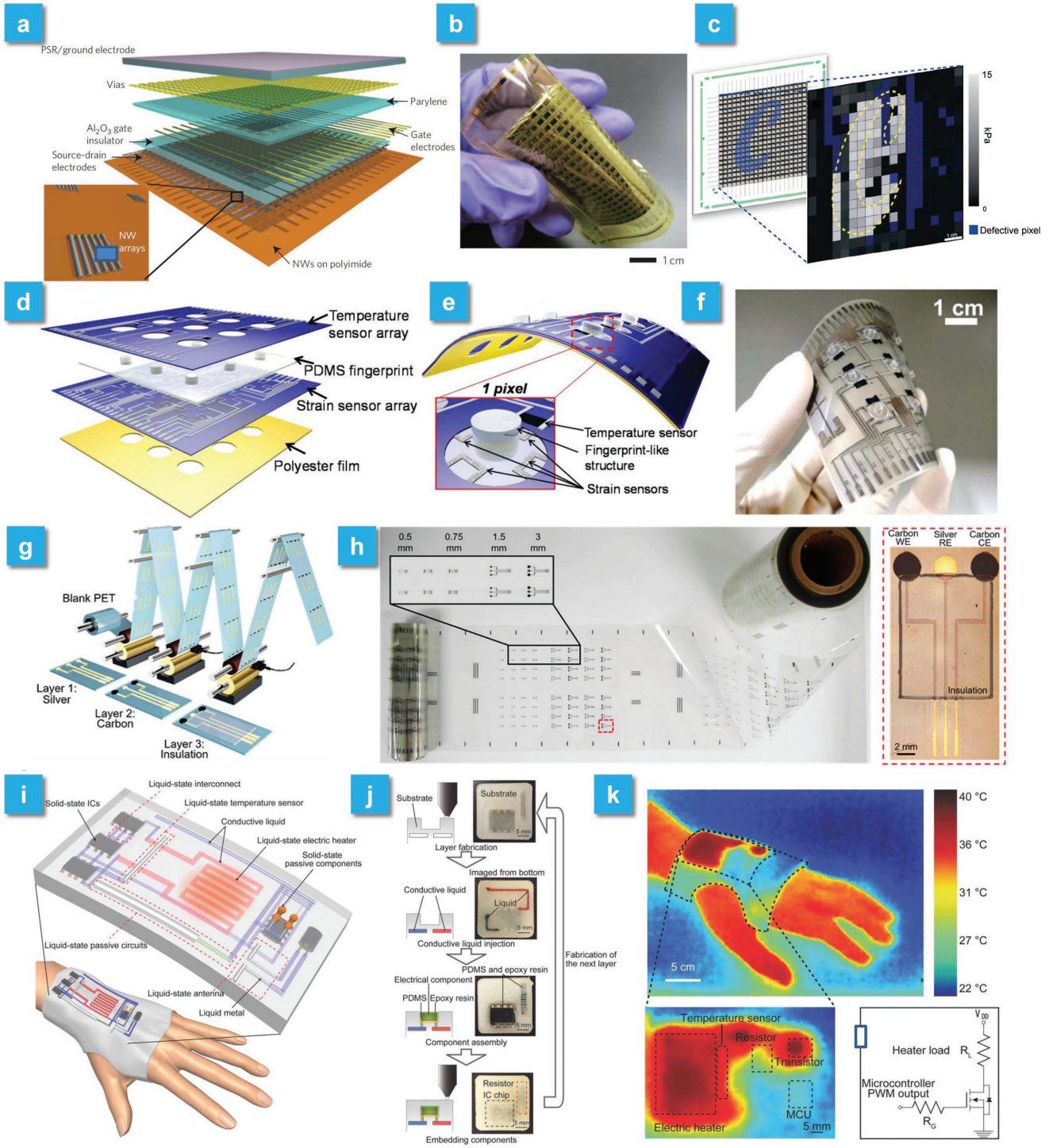


Figure 12. a) Schematic of the passive and active layers of NW E-skin. b) Optical photographs of a fully fabricated E-skin device under bending. c) Design layout of the sensor device and the corresponding 2D intensity profile obtained from experimental mapping of the pixel signals. a–c) Reproduced with permission.[22] Copyright 2010, Nature Publishing Group. d) Schematic of E-skin device with fingerprint-like structures. e) Schematic of the final E-skin device and an enlarged pixel with a fingerprint-like structure containing four strain sensors and a temperature sensor. f) Picture of a 3×3 array E-skin. d–f) Reproduced with permission.[182] Copyright 2014, American Chemical Society. g) Roll-to-roll gravure printing of biocompatible electrode arrays on flexible PET substrates. h) Roll-to-roll gravure printed electrodes on a 150 m roll of PET substrate and optical micrograph (right) of an array with 3 mm diameter electrodes. g,h) Reproduced with permission.[21] Copyright 2018, American Chemical Society. i) The multilayer schematic of a 3D printed smart object. j) The fabrication process flow of a given layer. k) Thermography of the worn glove while powered on and circuit diagram of the programmable power delivery to the heater based on the pulse width modulation (PWM) technique. i–k) Reproduced with permission.[183] Copyright 2016, John Wiley & Sons.

© 2019 WILEY-VCH Verlag GmbH & Co. KGaA, Weinheim

wearable sensor systems demand the judicious design of novel materials, logical layout of various units as well as rational packaging to make them survive in the unfriendly and tough ambient. Second, more efforts are encouraged to further integrate multiple sensors into self-healable materials so as to realize fully self-healable wearable E-skin systems, while simultaneously maintaining the high sensitivity of the flexible sensors. This will tremendously prolong the life-span of integrated wearable systems and probably make the unbreakable flexible devices come true. Third, although a great many of self-powered units integrated with flexible sensors have been developed based on smart energy conversion techniques, a completely battery-free human-friendly interactive electronic system integrated with multiple sensors has not been realized. It is still challenging to drive a plurality of sensors and concurrently perform the data processing, transmission, and visualization by current nanogenerators. The development of high-density, large-volume, yet lightweight energy storage modules coupled with more efficient energy conversion components is a potential strategy. In addition, for the large-scale fabrication of wearable electronics, ultrafast laser processing is an alternatively promising means to flexibly pattern the active sensing areas, allowing the formation of enhanced features of materials through laser-induced chemical reactions.[195–197] However, as the flexible sensor systems are usually composed of various units with different materials, the selection of laser wavelength, repetition rate, pulse durations, power density, processing speed, etc., should be carefully considered and explored for versatile wearable sensors. The effective settlement of these critical issues will render the ultimate realization of the most cutting-edge multifunctional skin-like electronic systems to benefit human beings.

Acknowledgements

This study was supported by JST PRESTO (JPMJPR17J5) and JSPS KAKENHI grants (JP17H04926 and JP18H05472). This article is part of the special series on Advanced Intelligent Systems that showcases the outstanding achievements of leading international researchers on intelligent systems.

Conflict of Interest

The authors declare no conflict of interest.

Keywords

electronic skin, flexible wearable sensors, multifunctionality, self-healable devices, self-powered systems

Received: November 16, 2018
Revised: December 6, 2018
Published online:

[1] Y. Lee, J. Park, S. Cho, Y. E. Shin, H. Lee, J. Kim, J. Myoung, S. Cho, S. Kang, C. Baig, H. Ko, *ACS Nano* **2018**, *12*, 4045.
[2] C. Bianchi, J. Loureiro, P. Duarte, J. Marques, J. Figueira, I. Ropio, I. Ferreira, *Adv. Mater. Technol.* **2016**, *1*, 1600077.
[3] R. C. Webb, A. P. Bonifas, A. Behnaz, Y. Zhang, K. J. Yu, H. Cheng, M. Shi, Z. Bian, Z. Liu, Y. S. Kim, W. H. Yeo, J. S. Park, J. Song, Y. Li, Y. Huang, A. M. Gorbach, J. A. Rogers, *Nat. Mater.* **2013**, *12*, 938.
[4] T. Q. Trung, N. E. Lee, *Adv. Mater.* **2016**, *28*, 4338.
[5] K. Takei, W. Honda, S. Harada, T. Arie, S. Akita, *Adv. Healthcare Mater.* **2015**, *4*, 487.
[6] S. Wang, J. Y. Oh, J. Xu, H. Tran, Z. Bao, *Acc. Chem. Res.* **2018**, *51*, 1033.
[7] T. Cheng, Y. Zhang, W. Y. Lai, W. Huang, *Adv. Mater.* **2015**, *27*, 3349.
[8] T. H. Chang, K. Li, H. Yang, P. Y. Chen, *Adv. Mater.* **2018**, *30*, 1802418.
[9] D. Qi, Z. Liu, W. R. Leow, X. Chen, *MRS Bull.* **2017**, *42*, 103.
[10] S. Nakata, M. Shiomi, Y. Fujita, T. Arie, S. Akita, K. Takei, *Nat. Electron.* **2018**, *1*, 596.
[11] X. Wang, L. Dong, H. Zhang, R. Yu, C. Pan, Z. L. Wang, *Adv. Sci.* **2015**, *2*, 1500169.
[12] J. Kim, M. Lee, H. J. Shim, R. Ghaffari, H. R. Cho, D. Son, Y. H. Jung, M. Soh, C. Choi, S. Jung, K. Chu, D. Jeon, S. T. Lee, J. H. Kim, S. H. Choi, T. Hyeon, D. H. Kim, *Nat. Commun.* **2014**, *5*, 5747.
[13] Y. Yang, W. Gao, *Chem. Soc. Rev.* **2018**, https://doi.org/10.1039/C7CS00730B.
[14] L. Xu, S. R. Gutbrod, Y. Ma, A. Petrossians, Y. Liu, R. C. Webb, J. A. Fan, Z. Yang, R. Xu, J. J. Whalen III, *Adv. Mater.* **2015**, *27*, 1731.
[15] C. Wang, X. Li, H. Hu, L. Zhang, Z. Huang, M. Lin, Z. Zhang, Z. Yin, B. Huang, H. Gong, *Nat. Biomed. Eng.* **2018**, *2*, 687.
[16] Q. Hua, J. Sun, H. Liu, R. Bao, R. Yu, J. Zhai, C. Pan, Z. L. Wang, *Nat. Commun.* **2018**, *9*, 244.
[17] S. Zhao, R. Zhu, *Adv. Mater.* **2017**, *29*, 1606151.
[18] Y. Yamamoto, S. Harada, D. Yamamoto, W. Honda, T. Arie, S. Akita, K. Takei, *Sci. Adv.* **2016**, *2*, e1601473.
[19] Y. J. Tan, J. Wu, H. Li, B. C. K. Tee, *ACS Appl. Mater. Interfaces* **2018**, *10*, 15331.
[20] C. Dagdeviren, Z. Li, Z. L. Wang, *Annu. Rev. Biomed. Eng.* **2017**, *19*, 85.
[21] M. Bariya, Z. Shahpar, H. Park, J. Sun, Y. Jung, W. Gao, H. Y. Y. Nyein, T. S. Liaw, L. C. Tai, Q. P. Ngo, M. Chao, Y. Zhao, M. Hettick, G. Cho, A. Javey, *ACS Nano* **2018**, *12*, 6978.
[22] K. Takei, T. Takahashi, J. C. Ho, H. Ko, A. G. Gillies, P. W. Leu, R. S. Fearing, A. Javey, *Nat. Mater.* **2010**, *9*, 821.
[23] C. Wang, D. Hwang, Z. Yu, K. Takei, J. Park, T. Chen, B. Ma, A. Javey, *Nat. Mater.* **2013**, *12*, 899.
[24] Y. Khan, D. Han, A. Pierre, J. Ting, X. Wang, C. M. Lochner, G. Bovo, N. Yaacobi-Gross, C. Newsome, R. Wilson, A. C. Arias, *Proc. Natl. Acad. Sci. USA* **2018**, *115*, E11015.
[25] W. Gao, S. Emaminejad, H. Y. Y. Nyein, S. Challa, K. Chen, A. Peck, H. M. Fahad, H. Ota, H. Shiraki, D. Kiriya, D. H. Lien, G. A. Brooks, R. W. Davis, A. Javey, *Nature* **2016**, *529*, 509.
[26] D. Son, J. Kang, O. Vardoulis, Y. Kim, N. Matsuhisa, J. Y. Oh, J. W. F. To, J. Mun, T. Katsumata, Y. Liu, A. F. McGuire, M. Krason, F. Molina-Lopez, J. Ham, U. Kraft, Y. Lee, Y. Yun, J. B. H. Tok, Z. Bao, *Nat. Nanotechnol.* **2018**, *13*, 1057.
[27] E. J. Markvicka, M. D. Bartlett, X. Huang, C. Majidi, *Nat. Mater.* **2018**, *17*, 618.
[28] M. A. Darabi, A. Khosrozadeh, R. Mbeleck, Y. Liu, Q. Chang, J. Jiang, J. Cai, Q. Wang, G. Luo, M. Xing, *Adv. Mater.* **2017**, *29*, 1700533.
[29] J. Yun, C. Song, H. Lee, H. Park, Y. R. Jeong, J. W. Kim, S. W. Jin, S. Y. Oh, L. Sun, G. Zi, J. S. Ha, *Nano Energy* **2018**, *49*, 644.
[30] S. Park, S. W. Heo, W. Lee, D. Inoue, Z. Jiang, K. Yu, H. Jinno, D. Hashizume, M. Sekino, T. Yokota, K. Fukuda, K. Tajima, T. Someya, *Nature* **2018**, *561*, 516.
[31] R. Cao, X. Pu, X. Du, W. Yang, J. Wang, H. Guo, S. Zhao, Z. Yuan, C. Zhang, C. Li, Z. L. Wang, *ACS Nano* **2018**, *12*, 5190.
[32] S. Han, C. Liu, H. Xu, D. Yao, K. Yan, H. Zheng, H.-J. Chen, X. Gui, S. Chu, C. Liu, *npj Flexible Electron.* **2018**, *2*, 16.

© 2019 WILEY-VCH Verlag GmbH & Co. KGaA, Weinheim

[33] X. Fan, N. Wang, F. Yan, J. Wang, W. Song, Z. Ge, *Adv. Mater. Technol.* **2018**, *3*, 1800030.
[34] S. Chen, R. Wu, P. Li, Q. Li, Y. Gao, B. Qian, F. Xuan, *ACS Appl. Mater. Interfaces* **2018**, *10*, 37760.
[35] X. Fang, J. Tan, Y. Gao, Y. Lu, F. Xuan, *Nanoscale* **2017**, *9*, 17948.
[36] S. Nakata, K. Kanao, S. Harada, T. Arie, S. Akita, K. Takei, *Phys. Status Solidi A* **2016**, *213*, 2345.
[37] L. Li, H. Xiang, Y. Xiong, H. Zhao, Y. Bai, S. Wang, F. Sun, M. Hao, L. Liu, T. Li, Z. Peng, J. Xu, T. Zhang, *Adv. Sci.* **2018**, *5*, 1800558.
[38] W. Tang, T. Yan, J. Ping, J. Wu, Y. Ying, *Adv. Mater. Technol.* **2017**, *2*, 1700021.
[39] K. Kanao, S. Harada, Y. Yamamoto, W. Honda, T. Arie, S. Akita, K. Takei, *RSC Adv.* **2015**, *5*, 30170.
[40] S. Ma, T. Ye, T. Zhang, Z. Wang, K. Li, M. Chen, J. Zhang, Z. Wang, S. Ramakrishna, L. Wei, *Adv. Mater. Technol.* **2018**, *3*, 1800033.
[41] Y. S. Rim, S. H. Bae, H. Chen, N. De Marco, Y. Yang, *Adv. Mater.* **2016**, *28*, 4415.
[42] M. Amjadi, K.-U. Kyung, I. Park, M. Sitti, *Adv. Funct. Mater.* **2016**, *26*, 1678.
[43] S. Lee, A. Reuveny, J. Reeder, S. Lee, H. Jin, Q. Liu, T. Yokota, T. Sekitani, T. Isoyama, Y. Abe, Z. Suo, T. Someya, *Nat. Nanotechnol.* **2016**, *11*, 472.
[44] K. Kanao, S. Nakata, T. Arie, S. Akita, K. Takei, *Mater. Horiz.* **2017**, *4*, 1079.
[45] D. Yamamoto, S. Nakata, K. Kanao, T. Arie, S. Akita, K. Takei, *Adv. Mater. Technol.* **2017**, *2*, 1700057.
[46] B. Zhu, H. Wang, Y. Liu, D. Qi, Z. Liu, H. Wang, J. Yu, M. Sherburne, Z. Wang, X. Chen, *Adv. Mater.* **2016**, *28*, 1559.
[47] K. Kanao, T. Arie, S. Akita, K. Takei, *J. Mater. Chem. C* **2016**, *4*, 9261.
[48] G. Casula, P. Cosseddu, A. Bonfiglio, *Adv. Electron. Mater.* **2015**, *1*, 1500234.
[49] S. H. Jo, T. Chang, I. Ebong, B. B. Bhadviya, P. Mazumder, W. Lu, *Nano Lett.* **2010**, *10*, 1297.
[50] B.-C. Zhang, H. Wang, Y. Zhao, F. Li, X.-M. Ou, B.-Q. Sun, X.-H. Zhang, *Nanoscale* **2016**, *8*, 2123.
[51] D. Y. Choi, M. H. Kim, Y. S. Oh, S.-H. Jung, J. H. Jung, H. J. Sung, H. W. Lee, H. M. Lee, *ACS Appl. Mater. Interfaces* **2017**, *9*, 1770.
[52] T. Yamada, Y. Hayamizu, Y. Yamamoto, Y. Yomogida, A. Izadi-Najafabadi, D. N. Futaba, K. Hata, *Nat. Nanotechnol.* **2011**, *6*, 296.
[53] A. Atalay, V. Sanchez, O. Atalay, D. M. Vogt, F. Haufe, R. J. Wood, C. J. Walsh, *Adv. Mater. Technol.* **2017**, *2*, 1700136.
[54] S. Ryu, P. Lee, J. B. Chou, R. Xu, R. Zhao, A. J. Hart, S.-G. Kim, *ACS Nano* **2015**, *9*, 5929.
[55] W. Honda, S. Harada, S. Ishida, T. Arie, S. Akita, K. Takei, *Adv. Mater.* **2015**, *27*, 4674.
[56] H. Yang, D. Qi, Z. Liu, B. K. Chandran, T. Wang, J. Yu, X. Chen, *Adv. Mater.* **2016**, *28*, 9175.
[57] W. Honda, S. Harada, T. Arie, S. Akita, K. Takei, *Adv. Funct. Mater.* **2014**, *24*, 3299.
[58] S. Harada, W. Honda, T. Arie, S. Akita, K. Takei, *ACS Nano* **2014**, *8*, 3921.
[59] D.-H. Kim, N. Lu, R. Ghaffari, Y.-S. Kim, S. P. Lee, L. Xu, J. Wu, R.-H. Kim, J. Song, Z. Liu, *Nat. Mater.* **2011**, *10*, 316.
[60] T. Yokota, Y. Inoue, Y. Terakawa, J. Reeder, M. Kaltenbrunner, T. Ware, K. Yang, K. Mabuchi, T. Murakawa, M. Sekino, W. Voit, T. Sekitani, T. Someya, *Proc. Natl. Acad. Sci. USA* **2015**, *112*, 14533.
[61] Y. Chen, B. Lu, Y. Chen, X. Feng, *Sci. Rep.* **2015**, *5*, 11505.
[62] C. Zhu, A. Chortos, Y. Wang, R. Pfattner, T. Lei, A. C. Hinckley, I. Pochorovski, X. Yan, J. W. F. To, J. Y. Oh, J. B. H. Tok, Z. Bao, B. Murmann, *Nat. Electron.* **2018**, *1*, 183.
[63] X. Ren, K. Pei, B. Peng, Z. Zhang, Z. Wang, X. Wang, P. K. Chan, *Adv. Mater.* **2016**, *28*, 4832.
[64] H. Ota, M. Chao, Y. Gao, E. Wu, L. C. Tai, K. Chen, Y. Matsuoka, K. Iwai, H. M. Fahad, W. Gao, H. Y. Y. Nyein, L. Lin, A. Javey, *ACS Sens.* **2017**, *2*, 990.
[65] M. S. Mannoor, H. Tao, J. D. Clayton, A. Sengupta, D. L. Kaplan, R. R. Naik, N. Verma, F. G. Omenetto, M. C. McAlpine, *Nat. Commun.* **2012**, *3*, 763.
[66] N. Kahn, O. Lavie, M. Paz, Y. Segev, H. Haick, *Nano Lett.* **2015**, *15*, 7023.
[67] A. Koh, D. K. Kang, Y. Xue, S. Lee, R. M. Pielak, J. Kim, T. Hwang, S. Min, A. Banks, P. Bastien, M. C. Manco, L. Wang, K. R. Ammann, K.-I. Jang, P. Won, S. Han, R. Ghaffari, U. Paik, M. J. Slepian, G. Balooch, Y. Huang, J. A. Rogers, *Sci. Transl. Med.* **2016**, *8*, 366ra165.
[68] M. Bariya, H. Y. Y. Nyein, A. Javey, *Nat. Electron.* **2018**, *1*, 160.
[69] A. J. Bandodkar, I. Jeerapan, J. Wang, *ACS Sens.* **2016**, *1*, 464.
[70] J. Choi, Y. Xue, W. Xia, T. R. Ray, J. T. Reeder, A. J. Bandodkar, D. Kang, S. Xu, Y. Huang, J. A. Rogers, *Lab Chip* **2017**, *17*, 2572.
[71] A. Martin, J. Kim, J. F. Kurniawan, J. R. Sempionatto, J. R. Moreto, G. Tang, A. S. Campbell, A. Shin, M. Y. Lee, X. Liu, J. Wang, *ACS Sens.* **2017**, *2*, 1860.
[72] H. Y. Y. Nyein, L. C. Tai, Q. P. Ngo, M. Chao, G. B. Zhang, W. Gao, M. Bariya, J. Bullock, H. Kim, H. M. Fahad, A. Javey, *ACS Sens.* **2018**, *3*, 944.
[73] S. Anastasova, B. Crewther, P. Bembnowicz, V. Curto, H. M. Ip, B. Rosa, G.-Z. Yang, *Biosens. Bioelectron.* **2017**, *93*, 139.
[74] S. Emaminejad, W. Gao, E. Wu, Z. A. Davies, H. Yin Yin Nyein, S. Challa, S. P. Ryan, H. M. Fahad, K. Chen, Z. Shahpar, S. Talebi, C. Milla, A. Javey, R. W. Davis, *Proc. Natl. Acad. Sci. USA* **2017**, *114*, 4625.
[75] H. Zhang, J. A. Rogers, *Adv. Opt. Mater.* **2018**, https://doi.org/10.1002/adom.201800936.
[76] A. Sourav, Z. Li, Z. Huang, V. D. Botcha, C. Hu, J. P. Ao, Y. Peng, H. C. Kuo, J. Wu, X. Liu, *Adv. Opt. Mater.* **2018**, *6*, 1800461.
[77] H. Ling, S. Liu, Z. Zheng, F. Yan, *Small Methods* **2018**, *2*, 1800070.
[78] C. Xie, F. Yan, *Small* **2017**, *13*, 1701822.
[79] C. M. Lochner, Y. Khan, A. Pierre, A. C. Arias, *Nat. Commun.* **2014**, *5*, 5745.
[80] T. Yokota, P. Zalar, M. Kaltenbrunner, H. Jinno, N. Matsuhisa, H. Kitanosako, Y. Tachibana, W. Yukita, M. Koizumi, T. Someya, *Sci. Adv.* **2016**, *2*, e1501856.
[81] H. Xu, J. Liu, J. Zhang, G. Zhou, N. Luo, N. Zhao, *Adv. Mater.* **2017**, *29*, 1700975.
[82] S. Park, K. Fukuda, M. Wang, C. Lee, T. Yokota, H. Jin, H. Jinno, H. Kimura, P. Zalar, N. Matsuhisa, S. Umezu, G. C. Bazan, T. Someya, *Adv. Mater.* **2018**, *30*, 1802359.
[83] K. Xu, Z. Wang, C. F. Tan, N. Kang, L. Chen, L. Ren, E. S. Thian, G. W. Ho, R. Ji, M. Hong, *ACS Appl. Mater. Interfaces* **2017**, *9*, 26341.
[84] A. Ameen, L. P. Hackett, S. Seo, F. K. Dar, M. R. Gartia, L. L. Goddard, G. L. Liu, *Adv. Opt. Mater.* **2017**, *5*, 1601051.
[85] S. Xu, L. Jiang, Y. Nie, J. Wang, H. Li, Y. Liu, W. Wang, G. Xu, X. Luo, *ACS Appl. Mater. Interfaces* **2018**, *10*, 26851.
[86] Z. Y. Li, *Adv. Opt. Mater.* **2018**, *6*, 1701097.
[87] A. Balčytis, Y. Nishijima, S. Krishnamoorthy, A. Kuchmizhak, P. R. Stoddart, R. Petruškevičius, S. Juodkazis, *Adv. Opt. Mater.* **2018**, *6*, 1800292.
[88] K. Xu, C. Zhang, T. H. Lu, P. Wang, R. Zhou, R. Ji, M. Hong, *Opto-Electron. Eng.* **2017**, *44*, 185.
[89] M. Chirumamilla, A. Chirumamilla, A. S. Roberts, R. P. Zaccaria, F. De Angelis, P. Kjær Kristensen, R. Krahne, S. I. Bozhevolnyi, K. Pedersen, A. Toma, *Adv. Opt. Mater.* **2017**, *5*, 1600836.
[90] K. Li, Y. Wang, K. Jiang, Y. Ren, Y. Dai, Y. Lu, P. Wang, *Nanotechnology* **2016**, *27*, 495402.
[91] X.-Y. Zhao, G. Wang, M. Hong, *Mater. Chem. Phys.* **2018**, *214*, 377.
[92] Z. Zuo, Y. Wen, S. Zhang, *Nanoscale* **2018**, *10*, 14039.

© 2019 WILEY-VCH Verlag GmbH & Co. KGaA, Weinheim

[93] K. Xu, H. Yan, C. F. Tan, Y. Lu, Y. Li, G. W. Ho, R. Ji, M. Hong, *Adv. Opt. Mater.* **2018**, *6*, 1701167.
[94] K. Xu, C. Zhang, R. Zhou, R. Ji, M. Hong, *Opt. Express* **2016**, *24*, 10352.
[95] B. Jin, J. He, J. Li, Y. Zhang, *Adv. Opt. Mater.* **2018**, *6*, 1800056.
[96] C.-W. Lee, H. Ko, S.-H. Chang, C.-C. Huang, *Green Chem.* **2018**, *20*, 5318.
[97] W.-E. Hong, I.-L. Hsu, S.-Y. Huang, C.-W. Lee, H. Ko, P.-J. Tsai, D.-B. Shieh, C.-C. Huang, *J. Mater. Chem. B* **2018**, *6*, 5689.
[98] J. Xu, Y. J. Zhang, H. Yin, H. L. Zhong, M. Su, Z. Q. Tian, J. F. Li, *Adv. Opt. Mater.* **2018**, *6*, 1701069.
[99] Y. Li, C. Chen, K. Willems, S. Kerman, L. Lagae, G. Groeseneken, T. Stakenborg, P. Van Dorpe, *Adv. Opt. Mater.* **2017**, *5*, 1600907.
[100] W. Chen, X. Gui, Y. Zheng, B. Liang, Z. Lin, C. Zhao, H. Chen, Z. Chen, X. Li, Z. Tang, *Adv. Opt. Mater.* **2017**, *5*, 1600715.
[101] L.-L. Qu, Y.-Y. Geng, Z.-N. Bao, S. Riaz, H. Li, *Microchim. Acta* **2016**, *183*, 1307.
[102] S. Park, J. Lee, H. Ko, *ACS Appl. Mater. Interfaces* **2017**, *9*, 44088.
[103] C. Li, J. Yu, S. Xu, S. Jiang, X. Xiu, C. Chen, A. Liu, T. Wu, B. Man, C. Zhang, *Adv. Mater. Technol.* **2018**, *3*, 1800174.
[104] Y. Wang, Y. Jin, X. Xiao, T. Zhang, H. Yang, Y. Zhao, J. Wang, K. Jiang, S. Fan, Q. Li, *Nanoscale* **2018**, *10*, 15195.
[105] N. Zhou, G. Meng, Z. Huang, Y. Ke, Q. Zhou, X. Hu, *Analyst* **2016**, *141*, 5864.
[106] Z. Wang, M. Li, W. Wang, M. Fang, Q. Sun, C. Liu, *Nano Res.* **2016**, *9*, 1148.
[107] E. Rodríguez-Sevilla, G. V. Vázquez, E. Morales-Narváez, *Adv. Opt. Mater.* **2018**, *6*, 1800548.
[108] Y. Liu, C. Deng, D. Yi, X. Wang, Y. Tang, Y. Wang, *Nanoscale* **2017**, *9*, 15901.
[109] E. H. Koh, C. Mun, C. Kim, S. G. Park, E. J. Choi, S. H. Kim, J. Dang, J. Choo, J. W. Oh, D. H. Kim, H. S. Jung, *ACS Appl. Mater. Interfaces* **2018**, *10*, 10388.
[110] J. Wu, S. Han, T. Yang, Z. Li, Z. Wu, X. Gui, K. Tao, J. Miao, L. K. Norford, C. Liu, F. Huo, *ACS Appl. Mater. Interfaces* **2018**, *10*, 19097.
[111] M. Ha, J. Park, Y. Lee, H. Ko, *ACS Nano* **2015**, *9*, 3421.
[112] N. T. Tien, S. Jeon, D. I. Kim, T. Q. Trung, M. Jang, B. U. Hwang, K. E. Byun, J. Bae, E. Lee, J. B. Tok, Z. Bao, N. E. Lee, J. J. Park, *Adv. Mater.* **2014**, *26*, 796.
[113] F. Zhang, Y. Zang, D. Huang, C. A. Di, D. Zhu, *Nat. Commun.* **2015**, *6*, 8356.
[114] S. Nakata, T. Arie, S. Akita, K. Takei, *ACS Sens.* **2017**, *2*, 443.
[115] M. Jung, K. Kim, B. Kim, H. Cheong, K. Shin, O. S. Kwon, J. J. Park, S. Jeon, *ACS Appl. Mater. Interfaces* **2017**, *9*, 26974.
[116] S. Zhao, R. Zhu, *Adv. Mater. Technol.* **2017**, *2*, 1700183.
[117] J. Kim, J. R. Sempionatto, S. Imani, M. C. Hartel, A. Barfidokht, G. Tang, A. S. Campbell, P. P. Mercier, J. Wang, *Adv. Sci.* **2018**, *5*, 1800880.
[118] T. Someya, Y. Kato, T. Sekitani, S. Iba, Y. Noguchi, Y. Murase, H. Kawaguchi, T. Sakurai, *Proc. Natl. Acad. Sci. USA* **2005**, *102*, 12321.
[119] C. Wang, K. Xia, M. Zhang, M. Jian, Y. Zhang, *ACS Appl. Mater. Interfaces* **2017**, *9*, 39484.
[120] Q. Gui, Y. He, N. Gao, X. Tao, Y. Wang, *Adv. Funct. Mater.* **2017**, *27*, 1702050.
[121] Y. Yamamoto, D. Yamamoto, M. Takada, H. Naito, T. Arie, S. Akita, K. Takei, *Adv. Healthcare Mater.* **2017**, *6*, 1700495.
[122] M. Kaltenbrunner, T. Sekitani, J. Reeder, T. Yokota, K. Kuribara, T. Tokuhara, M. Drack, R. Schwödiauer, I. Graz, S. Bauer-Gogonea, *Nature* **2013**, *499*, 458.
[123] A. Zucca, K. Yamagishi, T. Fujie, S. Takeoka, V. Mattoli, F. Greco, *J. Mater. Chem. C* **2015**, *3*, 6539.
[124] A. Chortos, Z. Bao, *Mater. Today* **2014**, *17*, 321.
[125] S. Lee, A. Reuveny, J. Reeder, S. Lee, H. Jin, Q. Liu, T. Yokota, T. Sekitani, T. Isoyama, Y. Abe, *Nat. Nanotechnol.* **2016**, *11*, 472.
[126] J. W. Jeong, M. K. Kim, H. Cheng, W. H. Yeo, X. Huang, Y. Liu, Y. Zhang, Y. Huang, J. A. Rogers, *Adv. Healthcare Mater.* **2014**, *3*, 642.
[127] R. Morgan, M. Patterson, M. Nimmo, *Acta Physiol. Scand.* **2004**, *182*, 37.
[128] H. Y. Nyein, W. Gao, Z. Shahpar, S. Emaminejad, S. Challa, K. Chen, H. M. Fahad, L. C. Tai, H. Ota, R. W. Davis, A. Javey, *ACS Nano* **2016**, *10*, 7216.
[129] S. Y. Oh, S. Y. Hong, Y. R. Jeong, J. Yun, H. Park, S. W. Jin, G. Lee, J. H. Oh, H. Lee, S.-S. Lee, *ACS Appl. Mater. Interfaces* **2018**, *10*, 13729.
[130] H. Lee, T. K. Choi, Y. B. Lee, H. R. Cho, R. Ghaffari, L. Wang, H. J. Choi, T. D. Chung, N. Lu, T. Hyeon, S. H. Choi, D. H. Kim, *Nat. Nanotechnol.* **2016**, *11*, 566.
[131] Y. Lee, J. Kim, H. Joo, M. S. Raj, R. Ghaffari, D.-H. Kim, *Adv. Mater. Technol.* **2017**, *2*, 1700053.
[132] B. J. Blaiszik, S. L. B. Kramer, S. C. Olugebefola, J. S. Moore, N. R. Sottos, S. R. White, *Annu. Rev. Mater. Res.* **2010**, *40*, 179.
[133] Y. Yang, M. W. Urban, *Chem. Soc. Rev.* **2013**, *42*, 7446.
[134] Y. J. Liu, W. T. Cao, M. G. Ma, P. Wan, *ACS Appl. Mater. Interfaces* **2017**, *9*, 25559.
[135] Y. Shi, M. Wang, C. Ma, Y. Wang, X. Li, G. Yu, *Nano Lett.* **2015**, *15*, 6276.
[136] Y. Li, S. Chen, M. Wu, J. Sun, *Adv. Mater.* **2012**, *24*, 4578.
[137] Y. Yang, B. Zhu, D. Yin, J. Wei, Z. Wang, R. Xiong, J. Shi, Z. Liu, Q. Lei, *Nano Energy* **2015**, *17*, 1.
[138] Y. Tao, Y. Chang, Y. Tao, Z. Yang, H. Wu, *Mater. Chem. Phys.* **2014**, *148*, 778.
[139] L. Han, X. Lu, M. Wang, D. Gan, W. Deng, K. Wang, L. Fang, K. Liu, C. W. Chan, Y. Tang, *Small* **2017**, *13*, 1601916.
[140] G. Cai, J. Wang, K. Qian, J. Chen, S. Li, P. S. Lee, *Adv. Sci.* **2017**, *4*, 1600190.
[141] T. Wu, B. Chen, *ACS Appl. Mater. Interfaces* **2016**, *8*, 24071.
[142] A. R. Karimi, A. Khodadadi, *ACS Appl. Mater. Interfaces* **2016**, *8*, 27254.
[143] T. P. Huynh, H. Haick, *Adv. Mater.* **2016**, *28*, 138.
[144] Y. Cao, T. G. Morrissey, E. Acome, S. I. Allec, B. M. Wong, C. Keplinger, C. Wang, *Adv. Mater.* **2017**, *29*, 1605099.
[145] B. C. Tee, C. Wang, R. Allen, Z. Bao, *Nat. Nanotechnol.* **2012**, *7*, 825.
[146] S. Wu, J. Li, G. Zhang, Y. Yao, G. Li, R. Sun, C. Wong, *ACS Appl. Mater. Interfaces* **2017**, *9*, 3040.
[147] Y. Han, X. Wu, X. Zhang, C. Lu, *ACS Appl. Mater. Interfaces* **2017**, *9*, 20106.
[148] Z. Lou, L. Li, L. Wang, G. Shen, *Small* **2017**, *13*, 1701791.
[149] Z. Wen, J. Fu, L. Han, Y. Liu, M. Peng, L. Zheng, Y. Zhu, X. Sun, Y. Zi, *J. Mater. Chem. C* **2018**, *6*, 11893.
[150] F.-R. Fan, Z.-Q. Tian, Z. L. Wang, *Nano Energy* **2012**, *1*, 328.
[151] A. Pal, H. E. Cuellar, R. Kuang, H. F. N. Caurin, D. Goswami, R. V. Martinez, *Adv. Mater. Technol.* **2017**, *2*, 1700130.
[152] Y. Cheng, X. Lu, K. Hoe Chan, R. Wang, Z. Cao, J. Sun, G. Wei Ho, *Nano Energy* **2017**, *41*, 511.
[153] X. He, Y. Zi, H. Yu, S. L. Zhang, J. Wang, W. Ding, H. Zou, W. Zhang, C. Lu, Z. L. Wang, *Nano Energy* **2017**, *39*, 328.
[154] Q. Zhou, J. G. Park, K. N. Kim, A. K. Thokchom, J. Bae, J. M. Baik, T. Kim, *Nano Energy* **2018**, *48*, 471.
[155] T. Chen, Q. Shi, M. Zhu, T. He, L. Sun, L. Yang, C. Lee, *ACS Nano* **2018**, *12*, 11561.
[156] H. Chen, Y. Xu, L. Bai, Y. Jiang, J. Zhang, C. Zhao, T. Li, H. Yu, G. Song, N. Zhang, Q. Gan, *Adv. Mater. Technol.* **2017**, *2*, 1700044.
[157] C. Lu, J. Chen, T. Jiang, G. Gu, W. Tang, Z. L. Wang, *Adv. Mater. Technol.* **2018**, *3*, 1800021.

© 2019 WILEY-VCH Verlag GmbH & Co. KGaA, Weinheim

[158] X. Pu, H. Guo, J. Chen, X. Wang, Y. Xi, C. Hu, Z. L. Wang, *Sci. Adv.* **2017**, *3*, e1700694.
[159] Z. Lin, J. Chen, X. Li, Z. Zhou, K. Meng, W. Wei, J. Yang, Z. L. Wang, *ACS Nano* **2017**, *11*, 8830.
[160] Q. Shi, H. Wang, T. Wang, C. Lee, *Nano Energy* **2016**, *30*, 450.
[161] D. Y. Park, D. J. Joe, D. H. Kim, H. Park, J. H. Han, C. K. Jeong, H. Park, J. G. Park, B. Joung, K. J. Lee, *Adv. Mater.* **2017**, *29*, 1702308.
[162] M. F. Dupont, D. R. MacFarlane, J. M. Pringle, *Chem. Commun.* **2017**, *53*, 6288.
[163] H. Zhou, P. Liu, *ACS Appl. Energy Mater.* **2018**, *1*, 1424.
[164] P. Yang, K. Liu, Q. Chen, X. Mo, Y. Zhou, S. Li, G. Feng, J. Zhou, *Angew. Chem., Int. Ed.* **2016**, *55*, 12050.
[165] X.-Q. Wang, C. F. Tan, K. H. Chan, K. Xu, M. Hong, S.-W. Kim, G. W. Ho, *ACS Nano* **2017**, *11*, 10568.
[166] X.-Q. Wang, C. F. Tan, K. H. Chan, X. Lu, L. Zhu, S. W. Kim, G. W. Ho, *Nat. Commun.* **2018**, *9*, 3438.
[167] T. Ding, L. Zhu, X.-Q. Wang, K. H. Chan, X. Lu, Y. Cheng, G. W. Ho, *Adv. Energy Mater.* **2018**, *8*, 1802397.
[168] L. Jin, Y. Zhang, Y. Yu, Z. Chen, Y. Li, M. Cao, Y. Che, J. Yao, *Adv. Opt. Mater.* **2018**, *6*, 1800639.
[169] K. Song, N. Ma, Y. Yang, *Adv. Mater. Technol.* **2017**, *2*, 1700221.
[170] H. Xue, Q. Yang, D. Wang, W. Luo, W. Wang, M. Lin, D. Liang, Q. Luo, *Nano Energy* **2017**, *38*, 147.
[171] H. Zheng, Y. Zi, X. He, H. Guo, Y. C. Lai, J. Wang, S. L. Zhang, C. Wu, G. Cheng, Z. L. Wang, *ACS Appl. Mater. Interfaces* **2018**, *10*, 14708.
[172] Y. Zi, L. Lin, J. Wang, S. Wang, J. Chen, X. Fan, P. K. Yang, F. Yi, Z. L. Wang, *Adv. Mater.* **2015**, *27*, 2340.
[173] J.-G. Sun, T.-N. Yang, C.-Y. Wang, L.-J. Chen, *Nano Energy* **2018**, *48*, 383.
[174] M.-H. You, X.-X. Wang, X. Yan, J. Zhang, W.-Z. Song, M. Yu, Z.-Y. Fan, S. Ramakrishna, Y.-Z. Long, *J. Mater. Chem. A* **2018**, *6*, 3500.
[175] J. H. Lee, K. Y. Lee, M. K. Gupta, T. Y. Kim, D. Y. Lee, J. Oh, C. Ryu, W. J. Yoo, C. Y. Kang, S. J. Yoon, *Adv. Mater.* **2014**, *26*, 765.
[176] P. Wang, Z. Liu, K. Xu, D. J. Blackwood, M. Hong, A. G. Aberle, R. Stangl, I. M. Peters, *IEEE J. Photovoltaics* **2017**, *7*, 493.
[177] H. Jinno, K. Fukuda, X. Xu, S. Park, Y. Suzuki, M. Koizumi, T. Yokota, I. Osaka, K. Takimiya, T. Someya, *Nat. Energy* **2017**, *2*, 780.
[178] A. Campana, T. Cramer, D. T. Simon, M. Berggren, F. Biscarini, *Adv. Mater.* **2014**, *26*, 3874.
[179] T. Someya, T. Sekitani, S. Iba, Y. Kato, H. Kawaguchi, T. Sakurai, *Proc. Natl. Acad. Sci. USA* **2004**, *101*, 9966.
[180] X. Wu, Y. Ma, G. Zhang, Y. Chu, J. Du, Y. Zhang, Z. Li, Y. Duan, Z. Fan, J. Huang, *Adv. Funct. Mater.* **2015**, *25*, 2138.
[181] Q. Li, L. N. Zhang, X. M. Tao, X. Ding, *Adv. Healthcare Mater.* **2017**, *6*, 1601371.
[182] S. Harada, K. Kanao, Y. Yamamoto, T. Arie, S. Akita, K. Takei, *ACS Nano* **2014**, *8*, 12851.
[183] H. Ota, S. Emaminejad, Y. Gao, A. Zhao, E. Wu, S. Challa, K. Chen, H. M. Fahad, A. K. Jha, D. Kiriya, W. Gao, H. Shiraki, K. Morioka, A. R. Ferguson, K. E. Healy, R. W. Davis, A. Javey, *Adv. Mater. Technol.* **2016**, *1*, 1600013.
[184] P. H. Lau, K. Takei, C. Wang, Y. Ju, J. Kim, Z. Yu, T. Takahashi, G. Cho, A. Javey, *Nano Lett.* **2013**, *13*, 3864.
[185] Z. Fan, J. C. Ho, T. Takahashi, R. Yerushalmi, K. Takei, A. C. Ford, Y.-L. Chueh, A. Javey, *Adv. Mater.* **2009**, *21*, 3730.
[186] T. Takahashi, K. Takei, J. C. Ho, Y.-L. Chueh, Z. Fan, A. Javey, *J. Am. Chem. Soc.* **2009**, *131*, 2102.
[187] C. Yeom, K. Chen, D. Kiriya, Z. Yu, G. Cho, A. Javey, *Adv. Mater.* **2015**, *27*, 1561.
[188] D. H. Kim, H. G. Yoo, S. M. Hong, B. Jang, D. Y. Park, D. J. Joe, J. H. Kim, K. J. Lee, *Adv. Mater.* **2016**, *28*, 8371.
[189] D. Li, W. Y. Lai, Y. Z. Zhang, W. Huang, *Adv. Mater.* **2018**, *30*, 1704738.
[190] K. Chen, W. Gao, S. Emaminejad, D. Kiriya, H. Ota, H. Y. Nyein, K. Takei, A. Javey, *Adv. Mater.* **2016**, *28*, 4397.
[191] W. Wu, *Nanoscale* **2017**, *9*, 7342.
[192] B.-H. Lu, H.-B. Lan, H.-Z. Liu, *Opto-Electron. Adv.* **2018**, *1*, 17000401.
[193] L. Li, Y. Bai, L. Li, S. Wang, T. Zhang, *Adv. Mater.* **2017**, *29*, 1702517.
[194] X. Su, H. Li, X. Lai, Z. Chen, X. Zeng, *ACS Appl. Mater. Interfaces* **2018**, *10*, 10587.
[195] Y. Yu, P. C. Joshi, J. Wu, A. Hu, *ACS Appl. Mater. Interfaces* **2018**, *10*, 34005.
[196] C. Lu, Y. Gao, G. Yu, M. Xu, J. Tan, F. Xuan, *Sens. Actuators, A* **2018**, *281*, 124.
[197] J. Kwon, H. Cho, Y. D. Suh, J. Lee, H. Lee, J. Jung, D. Kim, D. Lee, S. Hong, S. H. Ko, *Adv. Mater. Technol.* **2017**, *2*, 1600222.

© 2019 WILEY-VCH Verlag GmbH & Co. KGaA, Weinheim